Dinuclear Molybdenum(VI) Complexes Based on Flexible Succinyl and Adipoyl Dihydrazones

Edi Topić [1], Vladimir Damjanović [2], Katarina Pičuljan [1] and Mirta Rubčić[1,*]

1 Department of Chemistry, Faculty of Science, University of Zagreb, Horvatovac 102a, 10000 Zagreb, Croatia; edi.topic@chem.pmf.hr (E.T.); kpiculjan@chem.pmf.hr (K.P.)
2 Department of Chemistry and Biochemistry, School of Medicine, University of Zagreb, Šalata 3, 10000 Zagreb, Croatia; vladimir.damjanovic@mef.hr
* Correspondence: mirta@chem.pmf.hr; Tel.: +385-1-4606-374

Supporting Information

Contents

Reaction scheme

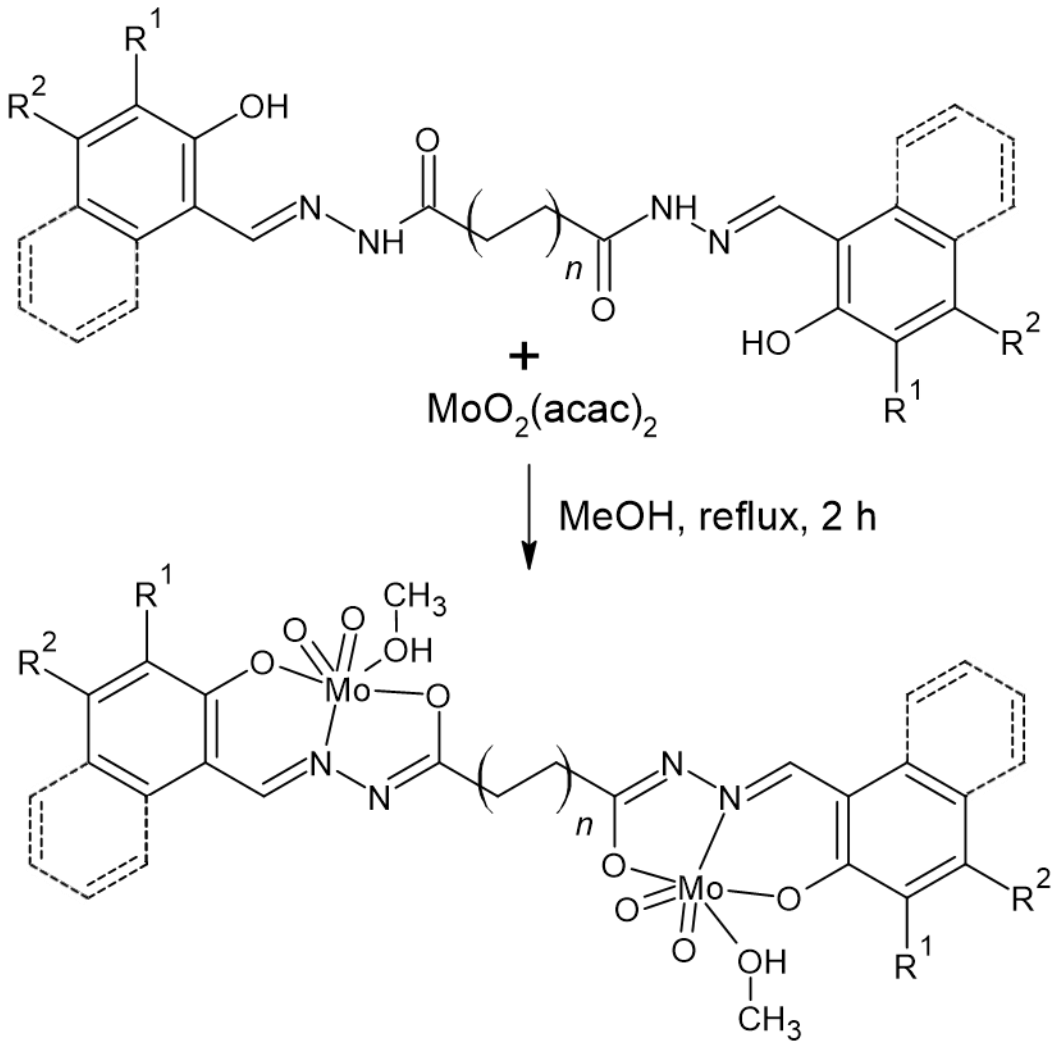

Compound	R^1	R^2	*n*	Additional ring
$[Mo_2O_4(MeOH)_2(L^1)]$	H	H	1	/
$[Mo_2O_4(MeOH)_2(L^2)]$	H	H	1	yes
$[Mo_2O_4(MeOH)_2(L^3)]$	OH	H	1	/
$[Mo_2O_4(MeOH)_2(L^4)]$	H	OH	1	/
$[Mo_2O_4(MeOH)_2(L^5)]$	H	H	2	/
$[Mo_2O_4(MeOH)_2(L^6)]$	H	H	2	yes
$[Mo_2O_4(MeOH)_2(L^7)]$	OH	H	2	/
$[Mo_2O_4(MeOH)_2(L^8)]$	H	OH	2	/

Scheme S1. Reaction scheme for synthesis of title compounds.

Crystallographic data

Table S1. Experimental and crystallographic data for complexes derived from succinyl dihydrazide.

Identifier	**$[Mo_2O_4(MeOH)_2(L^1)]\cdot 2MeOH$**	**$[Mo_2O_4(H_2O)_2(L^2)]$**	**$[Mo_2O_4(MeOH)_2(L^3)]\cdot 2MeOH$**	**$[Mo_2O_4(MeOH)_2(L^4)]\cdot 2MeOH$**
Empirical formula	$C_{22}H_{30}Mo_2N_4O_{12}$	$C_{26}H_{22}Mo_2N_4O_{10}$	$C_{22}H_{30}Mo_2N_4O_{14}$	$C_{11}H_{15}MoN_2O_7$
M_r	734.38	742.35	766.38	383.19
T/K	169.98(10)	169.98(10)	293(2)	293(2)
Crystal system	triclinic, yellow plate	monoclinic, yellow plate	triclinic, yellow plate	triclinic, yellow plate
Space group	$P\,\bar{1}$	$P\,1\,2_1/c\,1$	$P\,\bar{1}$	$P\,\bar{1}$
a/Å	7.3669(3)	13.4533(9)	7.3641(9)	7.5929(8)
b/Å	9.4297(4)	8.2944(3)	9.4730(12)	9.6293(7)
c/Å	10.1440(3)	13.3864(9)	11.1993(13)	10.0959(7)
α/°	98.417(3)	90	102.768(10)	96.570(6)
β/°	92.911(3)	116.282(8)	102.118(10)	92.887(7)
γ/°	98.726(4)	90	98.750(10)	99.382(7)
V/Å^3	687.10(5)	1339.33(16)	728.64(16)	721.70(11)
Z	1	2	1	2
ρ_{calc}/g cm^{-3}	1.775	1.841	1.747	1.763
μ/mm^{-1}	8.083	8.255	0.934	0.943
F(000)	370	740	386	386
Crystal size/mm^3	0.06×0.029×0.013	0.151×0.028×0.011	0.171×0.116×0.034	0.112×0.098×0.045
Radiation	CuKα (λ = 1.54184Å)	Cu Kα (λ = 1.54184Å)	MoKα (λ = 0.71073Å)	MoKα (λ = 0.71073Å)
2Θ range/°	8.836 to 160.336	7.328 to 159.756	8.834 to 50.0	8.648 to 49.994
Index ranges	$-9 \le h \le 9$, $-12 \le k \le 12$, $-12 \le l \le 12$	$-17 \le h \le 16$, $-10 \le k \le 8$, $-17 \le l \le 14$	$-8 \le h \le 8$, $-11 \le k \le 11$, $-13 \le l \le 13$	$-8 \le h \le 9$, $-11 \le k \le 11$, $-11 \le l \le 9$
Reflections collected	20329	9827	5359	5244
Independent reflections	2931 [R_{int} = 3.16%, R_{sigma} = 5.66 %]	2842 [R_{int} = 6.35%, R_{sigma} = 6.82 %]	2562 [R_{int} = 18.82%, R_{sigma} = 11.3 %]	2528 [R_{int} = 8.4%, R_{sigma} = 5.08 %]
Data/restraints/parameters	2931/-/186	2842/-/195	2562/-/201	2528/-/201
g_1, g_2 in w^a	0.0403, 0.9484	0.0553, 13.2979	0.0029, 0	0.0381, 0
Goodness–of–fit on F^2, S^b	1.168	1.047	0.920	1.023

Final R and wR^c values [$I \geq 2\sigma(I)$]	R_1 = 3.15%, wR_2 = 8.35%	R_1 = 6.01%, wR_2 = 15.09%	R_1 = 6.49%, wR_2 = 7.77%	R_1 = 4.89%, wR_2 = 9.1%
Final R and wR^c values [all data]	R_1 = 3.42%, wR_2 = 8.51%	R_1 = 7.91%, wR_2 = 16.02%	R_1 = 13.86%, wR_2 = 9.55%	R_1 = 7.32%, wR_2 = 9.93%
Largest diff. peak/hole / e Å^{-3}	0.541/–0.742	1.557/–1.618	0.511/–0.723	0.464/–0.482

[a] $w = 1/[\sigma F_o^2 + (g_1P)^2 + g_2P]$ where $P = (F_o^2 + 2F_c^2)/3$

[b] $S = \{\Sigma[w(F_o^2 - F_c^2)2]/(N_r - N_p)\}^{1/2}$ where N_r = number of independent reflections, N_p = number of refined parameters.

[c] $R = \Sigma||F_o| - |F_c|/\Sigma|F_o|$; $wR = \{\Sigma[w(F_o^2 - F_c^2)2]/\Sigma[w(F_o^2)2]\}^{1/2}$

Table S2. Experimental and crystallographic data for complexes derived from adipoyl dihydrazide.

Identifier	**$[Mo_2O_4(MeOH)_2(L^5)]$**	**$[Mo_2O_4(MeOH)_2(L^6)]$**	**$[Mo_2O_4(MeOH)_2(L^7)]$**	**$[Mo_2O_4(MeOH)_2(L^8)]\cdot 2MeOH$**
Empirical formula	$C_{22}H_{26}Mo_2N_4O_{10}$	$C_{30}H_{30}Mo_2N_4O_{10}$	$C_{22}H_{26}Mo_2N_4O_{12}$	$C_{24}H_{34}Mo_2N_4O_{14}$
M_r	698.35	798.46	730.35	794.43
T/K	169.99(10)	169.98(10)	169.98(10)	169.98(10)
Crystal system	triclinic, yellow block	monoclinic, yellow plate	monoclinic, yellow needle	monoclinic, yellow plate
Space group	$P\,\bar{1}$	$C\,1\,2/c\,1$	$C\,1\,2/c\,1$	$P\,1\,2_1/c\,1$
a/Å	7.0013(5)	16.287(3)	38.4604(9)	12.0854(4)
b/Å	8.3133(6)	8.1699(10)	7.7091(2)	13.5826(3)
c/Å	12.0124(7)	23.104(4)	8.9380(3)	10.1607(4)
α/°	80.805(5)	90	90	90
β/°	87.832(5)	103.952(17)	90.412(3)	114.635(4)
γ/°	68.817(7)	90	90	90
V/Å^3	643.40(8)	2983.7(8)	2650.00(13)	1516.08(10)
Z	1	4	4	2
ρ_{calc}/g cm^{-3}	1.802	1.777	1.831	1.740
μ/mm^{-1}	8.537	7.460	8.383	7.431
F(000)	350	1608	1464	804
Crystal size/mm^3	0.285×0.164×0.09	0.03×0.015×0.006	0.04×0.008×0.008	0.2×0.1×0.1
Radiation	CuKα (λ = 1.54184Å)	CuKα (λ = 1.54184Å)	CuKα (λ = 1.54184Å)	CuKα (λ = 1.54184Å)
2Θ range/°	7.456 to 160.598	7.886 to 95.344	9.198 to 159.43	8.048 to 160.088
Index ranges	$-8 \leq h \leq 8$, $-10 \leq k \leq 10$, $-15 \leq l \leq 13$	$-15 \leq h \leq 15$, $-3 \leq k \leq 7$, $-22 \leq l \leq 22$	$-48 \leq h \leq 32$, $-9 \leq k \leq 9$, $-11 \leq l \leq 11$	$-14 \leq h \leq 15$, $-17 \leq k \leq 17$, $-11 \leq l \leq 12$
Reflections collected	7726	4561	12114	11707
Independent reflections	2713 [R_{int} = 5.57%, R_{sigma} = 6.76 %]	1354 [R_{int} = 10.47%, R_{sigma} = 9.99 %]	2779 [R_{int} = 5.32%, R_{sigma} = 6.03 %]	3142 [R_{int} = 2.49%, R_{sigma} = 2.78 %]
Data/restraints/parameters	2713/-/177	1354/-/200	2779/-/188	3142/-/204

g_1, g_2 in w[a]	0.0863, 1.5578	0.0841, 0	0.0728, 14.2684	0.0397, 2.5789
Goodness–of–fit on F^2, S[b]	1.077	0.993	1.076	1.080
Final R and wR[c] values [$I \geq 2\sigma(I)$]	R_1 = 4.82%, wR_2 = 13.48%	R_1 = 5.8%, wR_2 = 12.72%	R_1 = 4.8%, wR_2 = 12.86%	R_1 = 3.1%, wR_2 = 8.11%
Final R and wR[c] values [all data]	R_1 = 4.97%, wR_2 = 13.6%	R_1 = 9.33%, wR_2 = 14.39%	R_1 = 6.37%, wR_2 = 13.7%	R_1 = 3.52%, wR_2 = 8.31%
Largest diff. peak/hole / e Å^{-3}	1.666/–1.018	1.066/–0.751	1.453/–1.265	0.550/–0.865

[a] $w = 1/[\sigma F_o^2 + (g_1P)^2 + g_2P]$ where $P = (F_o^2 + 2F_c^2)/3$

[b] $S = \{\Sigma[w(F_o^2 - F_c^2)2]/(N_r - N_p)\}^{1/2}$ where N_r = number of independent reflections, N_p = number of refined parameters.

[c] $R = \Sigma||F_o| - |F_c|/\Sigma|F_o|$; $wR = \{\Sigma[w(F_o^2 - F_c^2)2]/\Sigma[w(F_o^2)2]\}^{1/2}$

Table S3. Selected bond lengths in the crystal structures of complexes derived from succinyl dihydrazide.

$[Mo_2O_4(MeOH)_2(L^1)]\cdot 2MeOH$					
Atoms	Bond length/Å	Atoms	Bond length/Å	Atoms	Bond length/Å
C8–C9	1.501(4)	Mo1–O4	1.704(3)	O1–C2	1.349(3)
Mo1–N1	2.250(2)	Mo1–O5	2.299(2)	O2–C8	1.306(4)
Mo1–O1	1.9202(19)	N1–C7	1.288(4)	O5–C10	1.427(5)
Mo1–O2	2.016(2)	N1–N2	1.406(4)		
Mo1–O3	1.703(3)	N2–C8	1.305(4)		
$[Mo_2O_4(H_2O)_2(L^2)]$					
Atoms	Bond length/Å	Atoms	Bond length/Å	Atoms	Bond length/Å
C8–C9	1.485(11)	Mo1–O4	1.713(6)	O1–C2	1.352(10)
Mo1–N1	2.209(6)	Mo1–O5	2.321(7)	O2–C8	1.318(9)
Mo1–O1	1.908(6)	N1–C7	1.283(10)	O5–H5B	0.86(15)
Mo1–O2	2.022(6)	N1–N2	1.396(10)		
Mo1–O3	1.694(7)	N2–C8	1.303(10)		
$[Mo_2O_4(MeOH)_2(L^3)]\cdot 2MeOH$					
Atoms	Bond length/Å	Atoms	Bond length/Å	Atoms	Bond length/Å
Mo1–N1	2.247(6)	Mo1–O6	2.311(7)	O2–H2	0.81(5)
Mo1–O1	1.909(5)	N1–C7	1.278(10)	O3–C8	1.306(9)
Mo1–O3	2.016(5)	N1–N2	1.410(8)		
Mo1–O4	1.705(5)	O1–C2	1.346(8)		
Mo1–O5	1.704(4)	O2–C3	1.368(9)		
$[Mo_2O_4(MeOH)_2(L^4)]\cdot 2MeOH$					
Atoms	Bond length/Å	Atoms	Bond length/Å	Atoms	Bond length/Å
C1–C7	1.435(7)	Mo1–O5	1.712(3)	O1–C2	1.343(6)
Mo1–N1	2.229(4)	Mo1–O6	2.316(5)	O2–C4	1.343(6)
Mo1–O1	1.914(4)	N1–C7	1.280(6)	O2–H2	0.80(5)
Mo1–O3	2.006(3)	N1–N2	1.414(6)	O3–C8	1.313(6)
Mo1–O4	1.688(4)	N2–C8	1.300(7)		

Table S4. Selected bond lengths in the crystal structures of complexes derived from adipoyl dihydrazide.

$[Mo_2O_4(MeOH)_2(L^5)]$					
Atoms	Bond length/Å	Atoms	Bond length/Å	Atoms	Bond length/Å
C8–C9	1.494(7)	Mo1–O4	1.720(4)	O1–C2	1.350(6)
Mo1–N1	2.226(4)	Mo1–O5	2.375(4)	O2–C8	1.327(6)
Mo1–O1	1.926(3)	N1–C7	1.279(7)	O5–C11	1.414(8)
Mo1–O2	1.989(3)	N1–N2	1.410(6)	O5–H5	0.88(3)
Mo1–O3	1.692(4)	N2–C8	1.303(6)		
$[Mo_2O_4(MeOH)_2(L^6)]$					
Atoms	Bond length/Å	Atoms	Bond length/Å	Atoms	Bond length/Å
C8–C9	1.512(18)	Mo1–O4	1.724(8)	O1–C2	1.350(16)
Mo1–N1	2.232(10)	Mo1–O5	2.301(9)	O2–C8	1.284(14)
Mo1–O1	1.951(8)	N1–C7	1.289(16)	O5–C15	1.445(16)
Mo1–O2	2.016(9)	N1–N2	1.408(14)	O5–H005	0.88(5)
Mo1–O3	1.647(9)	N2–C8	1.314(16)		
$[Mo_2O_4(MeOH)_2(L^7)]$					
Atoms	Bond length/Å	Atoms	Bond length/Å	Atoms	Bond length/Å
Mo1–N1	2.262(5)	Mo1–O5	2.340(4)	O5–C11	1.406(8)
Mo1–O1	1.920(4)	N1–C7	1.282(7)	O5–H5	0.82(6)
Mo1–O2	2.010(4)	N1–N2	1.407(6)		
Mo1–O3	1.695(4)	O1–C2	1.335(7)		
$[Mo_2O_4(MeOH)_2(L^8)]\cdot 2MeOH$					
Atoms	Bond length/Å	Atoms	Bond length/Å	Atoms	Bond length/Å
C1–C7	1.435(5)	Mo1–O5	1.723(2)	O1–C2	1.351(4)
Mo1–N1	2.238(3)	Mo1–O6	2.320(2)	O2–C8	1.317(4)
Mo1–O1	1.925(2)	N1–C7	1.293(4)	O3–C4	1.352(5)
Mo1–O2	1.985(3)	N1–N2	1.412(4)		
Mo1–O4	1.694(3)	N2–C8	1.300(4)		

Table S5. Selected bond angles in the crystal structures of complexes derived from succinyl dihydrazide.

$[Mo_2O_4(MeOH)_2(L^1)]\cdot 2MeOH$					
Atoms	Bond angle/°	Atoms	Bond angle/°	Atoms	Bond angle/°
C2–C1–C7	123.6(3)	O1–Mo1–O4	103.42(11)	O5–Mo1–N1	75.65(9)
C6–C1–C7	117.8(3)	O1–Mo1–O5	80.96(10)	Mo1–N1–C7	128.1(2)
O1–C2–C1	122.7(3)	O2–Mo1–N1	71.49(9)	Mo1–N1–N2	115.2(2)
O1–C2–C3	117.4(3)	O2–Mo1–O3	96.16(12)	N2–N1–C7	116.6(2)
N1–C7–C1	123.4(3)	O2–Mo1–O4	96.97(11)	N1–N2–C8	109.1(3)
N2–C8–C9	120.0(3)	O2–Mo1–O5	78.82(10)	Mo1–O1–C2	135.78(18)
O2–C8–C9	116.4(2)	O3–Mo1–N1	93.30(12)	Mo1–O2–C8	120.49(17)
O2–C8–N2	123.6(3)	O3–Mo1–O4	105.51(14)	Mo1–O5–C10	125.0(2)
O1–Mo1–N1	81.94(9)	O3–Mo1–O5	168.81(13)		
O1–Mo1–O2	149.81(9)	O4–Mo1–N1	159.07(12)		
O1–Mo1–O3	99.50(12)	O4–Mo1–O5	85.14(12)		
$[Mo_2O_4(H_2O)_2(L^2)]$					
Atoms	Bond angle/°	Atoms	Bond angle/°	Atoms	Bond angle/°
C2–C1–C7	120.8(7)	O1–Mo1–O3	97.9(3)	O4–Mo1–O5	83.4(3)
C6–C1–C7	120.5(7)	O1–Mo1–O4	104.6(3)	O5–Mo1–N1	75.5(2)
O1–C2–C1	123.0(7)	O1–Mo1–O5	79.5(3)	Mo1–N1–C7	129.0(6)
O1–C2–C3	116.2(7)	O2–Mo1–N1	71.8(2)	Mo1–N1–N2	115.9(5)
N1–C7–C1	123.9(7)	O2–Mo1–O3	97.8(3)	N2–N1–C7	115.2(6)
N2–C8–C9	120.3(7)	O2–Mo1–O4	95.9(3)	N1–N2–C8	110.3(6)
O2–C8–C9	118.0(7)	O2–Mo1–O5	80.9(2)	Mo1–O1–C2	134.4(5)
O2–C8–N2	121.7(7)	O3–Mo1–N1	95.5(3)	Mo1–O2–C8	120.2(5)
C8–C9–C9_a	111.6(6)	O3–Mo1–O4	105.8(3)	Mo1–O5–H5B	115(11)
O1–Mo1–N1	80.9(2)	O3–Mo1–O5	170.9(2)		
O1–Mo1–O2	149.7(2)	O4–Mo1–N1	156.9(3)		
$[Mo_2O_4(MeOH)_2(L^3)]\cdot 2MeOH$					
Atoms	Bond angle/°	Atoms	Bond angle/°	Atoms	Bond angle/°
C2–C1–C7	121.5(7)	O1–Mo1–O3	149.1(2)	O5–Mo1–O6	85.2(2)
C6–C1–C7	120.2(6)	O1–Mo1–O4	99.4(2)	O6–Mo1–N1	76.6(2)
O1–C2–C1	123.4(6)	O1–Mo1–O5	105.2(2)	Mo1–N1–C7	126.8(5)
O1–C2–C3	117.2(6)	O1–Mo1–O6	80.3(2)	Mo1–N1–N2	115.5(4)
O2–C3–C2	120.7(7)	O3–Mo1–N1	71.5(2)	N2–N1–C7	117.6(6)
O2–C3–C4	118.4(7)	O3–Mo1–O4	96.9(2)	N1–N2–C8	108.8(5)
N1–C7–C1	125.3(6)	O3–Mo1–O5	95.4(2)	Mo1–O1–C2	134.9(4)
N2–C8–C9	120.5(6)	O3–Mo1–O6	78.7(2)	C3–O2–H2	102(7)
O3–C8–C9	116.0(6)	O4–Mo1–N1	92.2(2)	Mo1–O3–C8	120.7(5)
O3–C8–N2	123.5(7)	O4–Mo1–O5	105.7(2)	Mo1–O6–C10	125.7(5)
C8–C9–C9_a	113.2(6)	O4–Mo1–O6	168.7(2)	Mo1–O6–H6	123(6)
O1–Mo1–N1	81.8(2)	O5–Mo1–N1	159.1(2)		
$[Mo_2O_4(MeOH)_2(L^4)]\cdot 2MeOH$					

Atoms	Bond angle/°	Atoms	Bond angle/°	Atoms	Bond angle/°
C2–C1–C7	122.6(4)	O1–Mo1–O3	150.37(15)	O5–Mo1–O6	83.71(16)
C6–C1–C7	120.2(5)	O1–Mo1–O4	98.73(17)	O6–Mo1–N1	75.42(15)
O1–C2–C1	121.8(4)	O1–Mo1–O5	102.26(15)	Mo1–N1–C7	128.1(3)
O1–C2–C3	118.0(4)	O1–Mo1–O6	80.01(15)	Mo1–N1–N2	115.5(3)
O2–C4–C3	123.2(5)	O3–Mo1–N1	71.85(13)	N2–N1–C7	116.5(4)
O2–C4–C5	117.0(4)	O3–Mo1–O4	96.91(17)	N1–N2–C8	108.9(4)
N1–C7–C1	124.7(5)	O3–Mo1–O5	97.30(15)	Mo1–O1–C2	136.3(3)
N2–C8–C9	120.7(4)	O3–Mo1–O6	80.27(15)	C4–O2–H2	112(5)
O3–C8–C9	116.0(5)	O4–Mo1–N1	94.65(18)	Mo1–O3–C8	120.4(3)
O3–C8–N2	123.4(5)	O4–Mo1–O5	106.15(19)	Mo1–O6–C10	126.1(4)
C8–C9–C9_a	113.3(4)	O4–Mo1–O6	170.07(17)	Mo1–O6–H6	111(5)
O1–Mo1–N1	81.91(14)	O5–Mo1–N1	157.73(18)		

Table S6. Selected bond angles in the crystal structures of complexes derived from adipoyl dihydrazide.

$[Mo_2O_4(MeOH)_2(L^5)]$					
Atoms	Bond angle/°	Atoms	Bond angle/°	Atoms	Bond angle/°
C2–C1–C7	123.2(5)	O1–Mo1–O4	103.19(17)	O5–Mo1–N1	75.74(14)
C6–C1–C7	118.5(4)	O1–Mo1–O5	79.51(14)	Mo1–N1–C7	128.9(3)
O1–C2–C1	121.8(4)	O2–Mo1–N1	72.13(15)	Mo1–N1–N2	115.5(3)
O1–C2–C3	117.4(5)	O2–Mo1–O3	98.52(17)	N2–N1–C7	115.5(4)
N1–C7–C1	123.2(5)	O2–Mo1–O4	95.63(17)	N1–N2–C8	108.8(4)
N2–C8–C9	120.4(5)	O2–Mo1–O5	77.56(14)	Mo1–O1–C2	135.0(3)
O2–C8–C9	116.7(4)	O3–Mo1–N1	94.33(18)	Mo1–O2–C8	120.2(3)
O2–C8–N2	123.0(4)	O3–Mo1–O4	105.78(19)	C11–O5–H5	107(3)
O1–Mo1–N1	81.43(15)	O3–Mo1–O5	170.00(18)	Mo1–O5–C11	127.3(4)
O1–Mo1–O2	148.44(15)	O4–Mo1–N1	157.98(15)	Mo1–O5–H5	122(2)
O1–Mo1–O3	100.38(17)	O4–Mo1–O5	83.88(16)		
$[Mo_2O_4(MeOH)_2(L^6)]$					
Atoms	Bond angle/°	Atoms	Bond angle/°	Atoms	Bond angle/°
C2–C1–C7	124.4(12)	O1–Mo1–O4	103.8(4)	Mo1–N1–C7	128.8(8)
C6–C1–C7	117.3(12)	O1–Mo1–O5	80.2(3)	Mo1–N1–N2	115.3(7)
O1–C2–C1	121.9(12)	O2–Mo1–N1	71.6(3)	N2–N1–C7	115.9(10)
O1–C2–C3	116.1(11)	O2–Mo1–O3	99.8(4)	N1–N2–C8	108.2(9)
N1–C7–C1	120.7(11)	O2–Mo1–O4	97.0(4)	Mo1–O1–C2	130.5(8)
N2–C8–C9	119.2(11)	O2–Mo1–O5	79.2(3)	Mo1–O2–C8	120.1(8)
O2–C8–C9	116.6(11)	O3–Mo1–N1	96.1(4)	C15–O5–H5	108(4)
O2–C8–N2	124.2(12)	O3–Mo1–O4	106.3(4)	Mo1–O5–C15	129.5(7)
C8–C9–C10	113.0(11)	O3–Mo1–O5	171.8(3)	Mo1–O5–H5	121(4)
O1–Mo1–N1	80.0(4)	O4–Mo1–N1	156.5(4)		

O1–Mo1–O2	148.1(3)	O4–Mo1–O5	81.8(4)		
O1–Mo1–O3	97.2(4)	O5–Mo1–N1	75.9(3)		
$[Mo_2O_4(MeOH)_2(L^7)]$					
Atoms	Bond angle/°	Atoms	Bond angle/°	Atoms	Bond angle/°
C2–C1–C7	122.0(5)	O1–Mo1–O4	105.44(19)	Mo1–N1–C7	129.1(4)
C6–C1–C7	119.2(5)	O1–Mo1–O5	77.73(17)	Mo1–N1–N2	114.1(3)
O1–C2–C1	123.7(5)	O2–Mo1–N1	71.83(16)	N2–N1–C7	116.8(5)
O1–C2–C3	116.6(5)	O2–Mo1–O3	99.24(18)	N1–N2–C8	109.8(4)
N1–C7–C1	123.5(5)	O2–Mo1–O4	94.81(18)	Mo1–O1–C2	135.0(4)
N2–C8–C9	121.1(5)	O2–Mo1–O5	79.64(15)	Mo1–O2–C8	119.7(3)
O2–C8–C9	115.9(5)	O3–Mo1–N1	93.30(17)	C11–O5–H5	106(5)
O2–C8–N2	123.0(5)	O3–Mo1–O4	105.5(2)	Mo1–O5–C11	128.8(4)
C8–C9–C10	112.7(4)	O3–Mo1–O5	170.17(17)	Mo1–O5–H5	125(5)
O1–Mo1–N1	80.89(16)	O4–Mo1–N1	158.68(18)		
O1–Mo1–O2	147.76(16)	O4–Mo1–O5	84.37(18)		
O1–Mo1–O3	99.2(2)	O5–Mo1–N1	77.03(16)		
$[Mo_2O_4(MeOH)_2(L^8)]\cdot 2MeOH$					
Atoms	Bond angle/°	Atoms	Bond angle/°	Atoms	Bond angle/°
C2–C1–C7	123.8(3)	O1–Mo1–O2	148.33(9)	O5–Mo1–O6	86.20(11)
C6–C1–C7	119.0(3)	O1–Mo1–O4	97.99(11)	O6–Mo1–N1	76.82(9)
O1–C2–C1	122.0(3)	O1–Mo1–O5	105.21(10)	Mo1–N1–C7	127.3(2)
O1–C2–C3	116.9(3)	O1–Mo1–O6	77.13(10)	Mo1–N1–N2	115.35(19)
O3–C4–C3	122.0(3)	O2–Mo1–N1	71.56(9)	N2–N1–C7	117.2(3)
O3–C4–C5	118.0(3)	O2–Mo1–O4	99.57(11)	N1–N2–C8	108.8(3)
N1–C7–C1	122.9(3)	O2–Mo1–O5	95.21(10)	Mo1–O1–C2	131.42(18)
N2–C8–C9	124.1(3)	O2–Mo1–O6	80.42(9)	Mo1–O2–C8	121.5(2)
O2–C8–C9	113.2(3)	O4–Mo1–N1	91.95(11)	Mo1–O6–C11	129.4(2)
O2–C8–N2	122.7(3)	O4–Mo1–O5	105.48(12)		
C8–C9–C10	116.6(3)	O4–Mo1–O6	168.23(11)		
O1–Mo1–N1	81.72(9)	O5–Mo1–N1	159.86(11)		

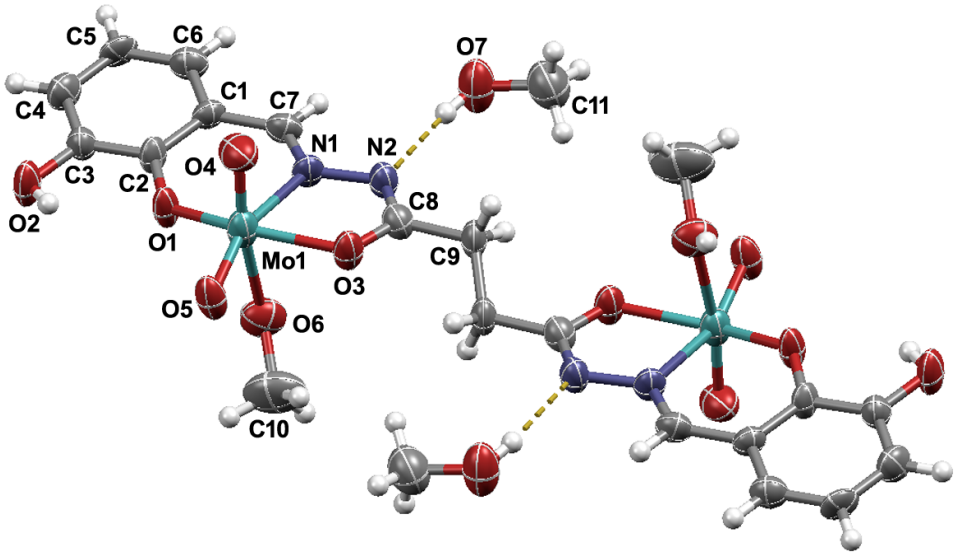

(a)

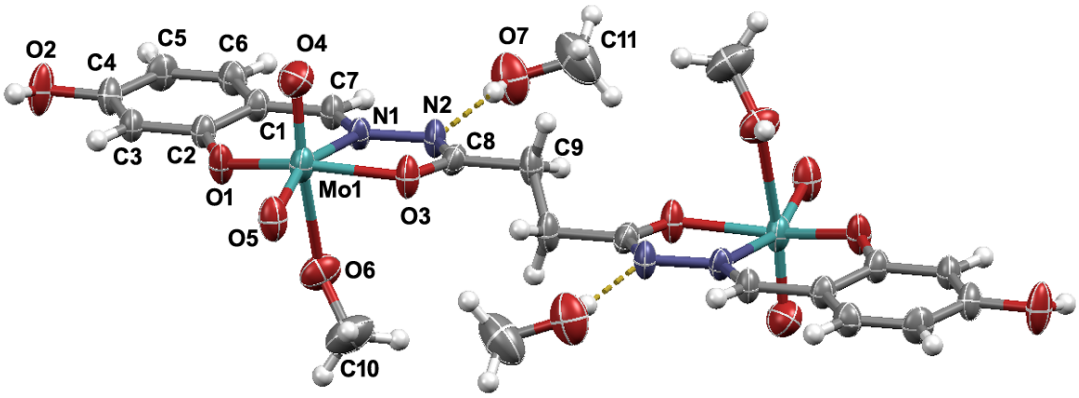

(b)

Figure S1. Molecular structures of: (a) **$[Mo_2O_4(MeOH)_2(L^3)]\cdot 2MeOH$** and **(**b) **$[Mo_2O_4(MeOH)_2(L^4)]\cdot 2MeOH$** with the atom numbering schemes. The central aliphatic C2 fragments of molecules lie on the inversion center. In (a) and (b) displacement ellipsoids are drawn at the 50% probability level, while the hydrogen atoms are presented as spheres of arbitrary small radii. Hydrogen bonds are highlighted by yellow dashed lines.

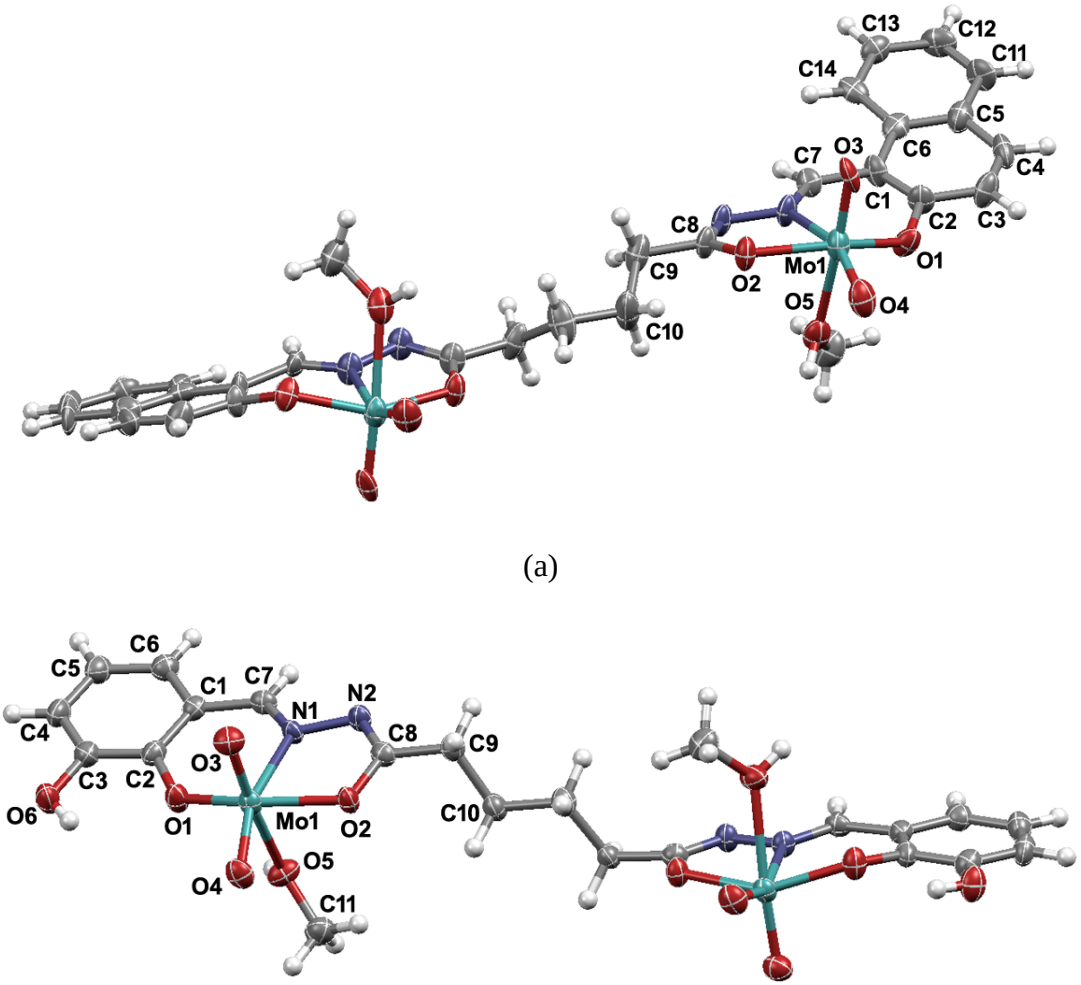

Figure S2. Molecular structures of: (a) **[$Mo_2O_4(MeOH)_2(L^6)$]** and **(**b) **[$Mo_2O_4(MeOH)_2(L^7)$]·2MeOH** with the atom numbering schemes. The central aliphatic C2 fragments of molecules lie on the inversion center. In (a) and (b) displacement ellipsoids are drawn at the 50% probability level, while the hydrogen atoms are presented as spheres of arbitrary small radii. Hydrogen bonds are highlighted by yellow dashed lines.

Table S7. Hydrogen bond parameters in the crystal structures of prepared complexes.

D–H···A	D-H	H···A	D···A	∠D–H···A	Symmetry code
$[Mo_2O_4(MeOH)_2(L^1)]\cdot 2MeOH$					
O5–H5···O6	0.84	1.83	2.670(4)	172	*x*, *y*, *z*
O6–H6A···N2	0.84	2.04	2.882(4)	179	1–*x*, 1–*y*, 1–*z*
C6–H6···O3	0.95	2.56	3.244(4)	129	2–*x*, 1–*y*, 1–*z*
C10–H10B···O3	0.98	2.47	3.314(5)	144	–1+*x*, *y*, *z*
$[Mo_2O_4(H_2O)_2(L^2)]$					
O5–H5A···N2	0.87	1.89	2.754(9)	172	1–*x*, –1/2+*y*, 3/2–*z*
O5–H5B···O4	0.86(15)	1.99(15)	2.822(9)	163(12)	1–*x*, 1/2+*y*, 3/2–*z*
C3–H3···O3	0.95	2.51	3.310(10)	142	*x*, 1/2–*y*, 1/2+*z*
C9–H9B···O4	0.99	2.49	3.378(9)	149	*x*, 1/2–*y*, –1/2+*z*
$[Mo_2O_4(MeOH)_2(L^3)]\cdot 2MeOH$					
O6–H6···O7	0.82(8)	1.87(7)	2.680(9)	172(7)	*x*, *y*, *z*
O7–H7A···N2	0.81(4)	2.16(6)	2.941(8)	162(9)	2–*x*, 1–*y*, 1–*z*
C10–H10B···O4	0.96	2.35	3.251(11)	156	1+*x*, *y*, *z*
$[Mo_2O_4(MeOH)_2(L^4)]\cdot 2MeOH$					
O2–H2···O5	0.80(5)	1.94(5)	2.737(5)	177(8)	–*x*, 1–*y*, 2–*z*
O6–H6···O7	0.81(5)	1.89(5)	2.671(6)	163(6)	*x*, *y*, *z*
O7–H7A···N2	0.81(5)	2.08(5)	2.878(6)	168(6)	1–*x*, 1–*y*, 1–*z*
C6–H6A···O4	0.93	2.60	3.203(6)	123	–*x*, 1–*y*, 1–*z*
$[Mo_2O_4(MeOH)_2(L^5)]$					
O5–H5···O4	0.88(8)	1.88(2)	2.728(5)	164(4)	2–*x*, 1–*y*, 1–*z*
C6–H6···O3	0.95	2.53	3.360(7)	146	–1+*x*, *y*, *z*
C9–H9A···O1	0.99	2.58	3.464(6)	148	*x*, –1+*y*, *z*
$[Mo_2O_4(MeOH)_2(L^6)]$					
O5–H5···N2	0.88(5)	1.91(5)	2.762(12)	165(9)	1/2–*x*, –1/2+*y*, 1/2–*z*
C7–H7···O4	0.95	2.60	3.525(14)	165	*x*, 1+*y*, *z*
C14–H14···O4	0.95	2.55	3.300(15)	136	*x*, 1+*y*, *z*
$[Mo_2O_4(MeOH)_2(L^7)]$					
O5–H5···N2	0.82(6)	1.96(6)	2.770(6)	169(6)	*x*, 1–*y*, –1/2+*z*
C4–H4···O6	0.95	2.47	3.417(7)	173	1/2–*x*, 1/2–*y*, –*z*
C7–H7···O4	0.95	2.50	3.306(7)	142	*x*, 1+*y*, *z*
C9–H9A···O4	0.99	2.56	3.293(7)	131	*x*, –*y*, 1/2+*z*
C11–H11C···O2	0.98	2.36	3.285(8)	156	*x*, –*y*, –1/2+*z*
$[Mo_2O_4(MeOH)_2(L^8)]\cdot 2MeOH$					
O3–H3···O5	0.84	1.92	2.757(3)	171	1–*x*, 1–*y*, 1–*z*
O6–H6···O7	0.84	1.80	2.627(3)	167	*x*, *y*, *z*
O7–H7A···N2	0.84	2.03	2.847(4)	163	*x*, 1/2–*y*, –1/2+*z*
C11–H11B···O2	0.98	2.42	3.248(5)	142	–*x*, 1–*y*, 1–*z*

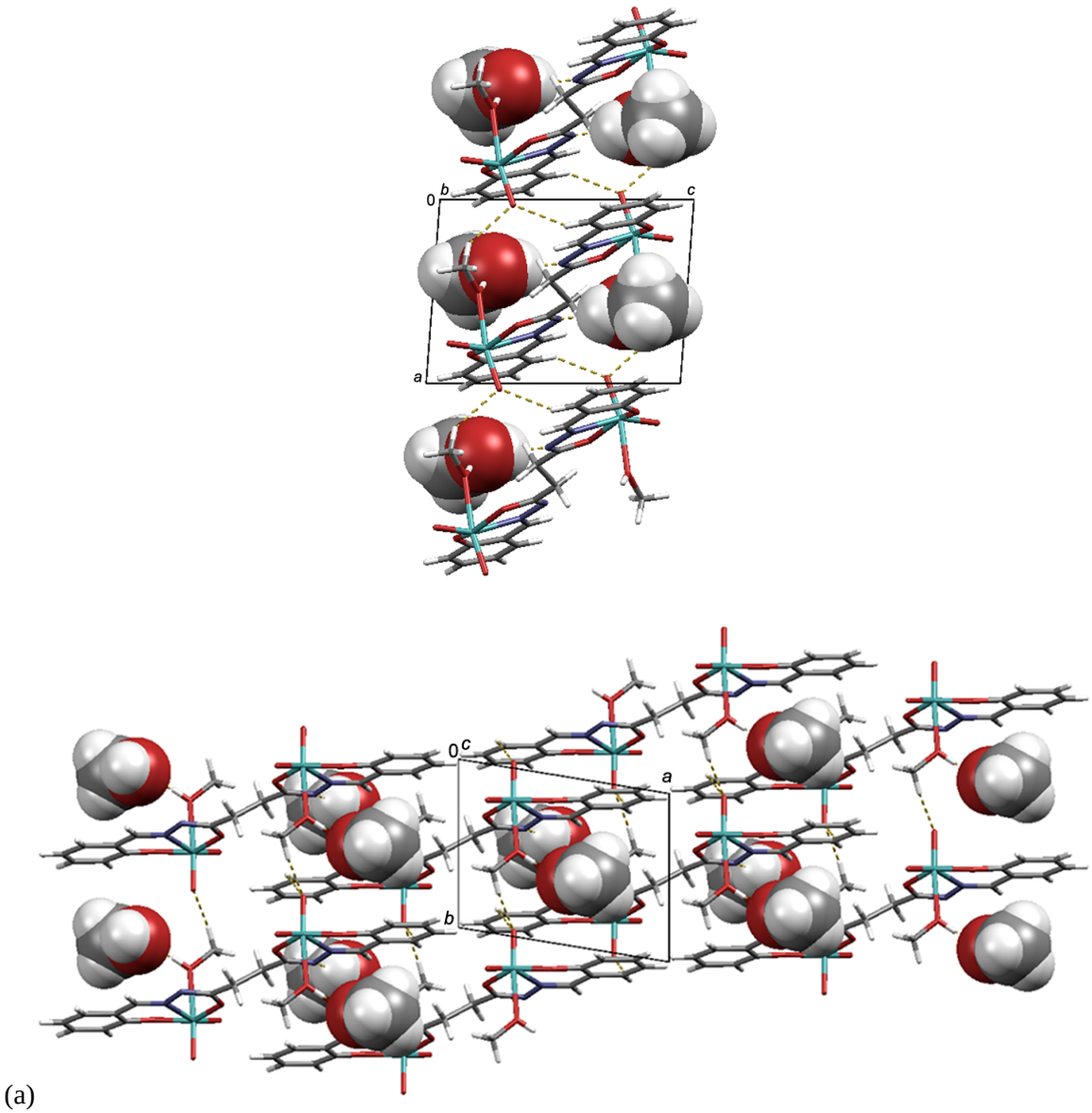

(a)

(b)

Figure S3. Fragment of crystal structure in **[$Mo_2O_4(MeOH)_2(L^1)$]·2MeOH** shown down the: (a) *b*-axis, and (b) *c*-axis. Crystal methanol molecules are shown in a spacefill style.

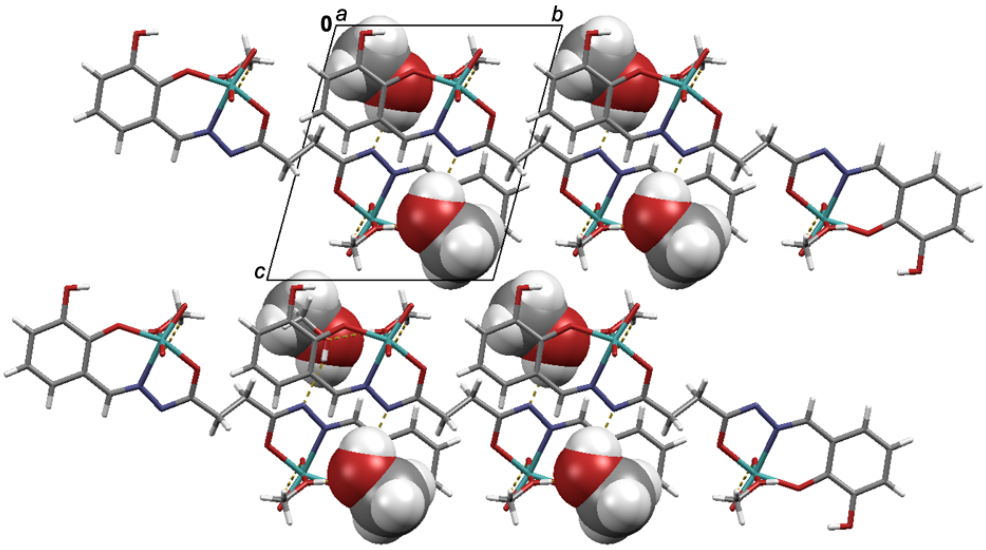

(a)

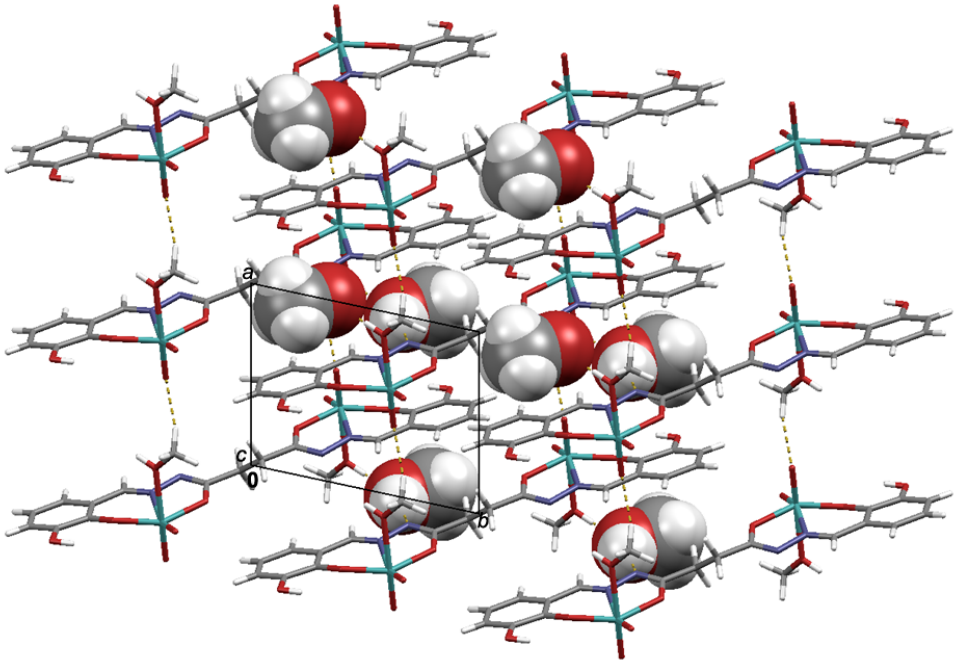

(b)

Figure S4. Fragment of crystal structure in **[$Mo_2O_4(MeOH)_2(L^3)$]·2MeOH** shown down the: (a) *a*-axis, and (b) *c*-axis.

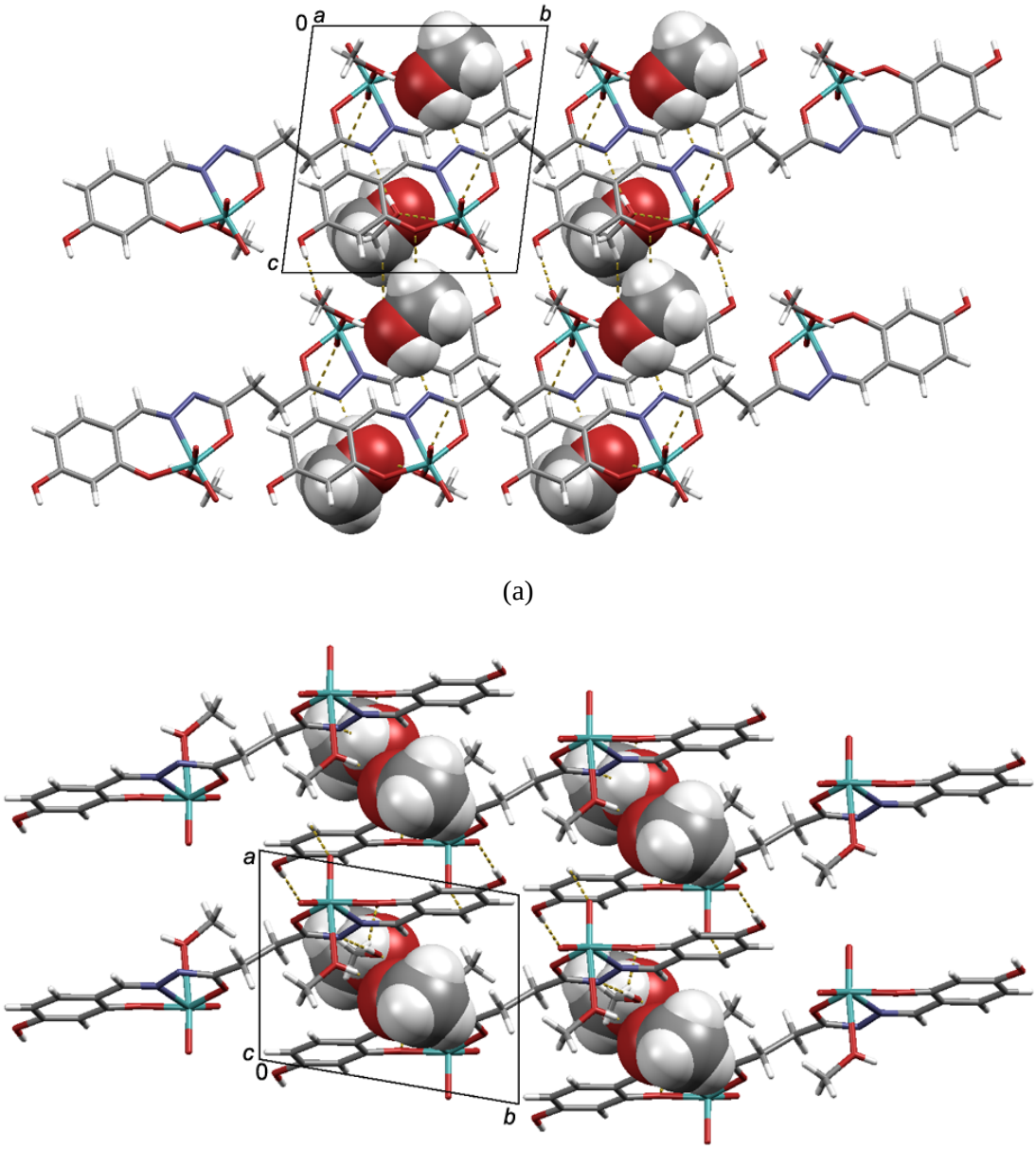

(a)

(b)

Figure S5. Fragment of crystal structure in **$[Mo_2O_4(MeOH)_2(L^4)]\cdot 2MeOH$** shown down the: (a) *a*-axis, and (b) *c*-axis.

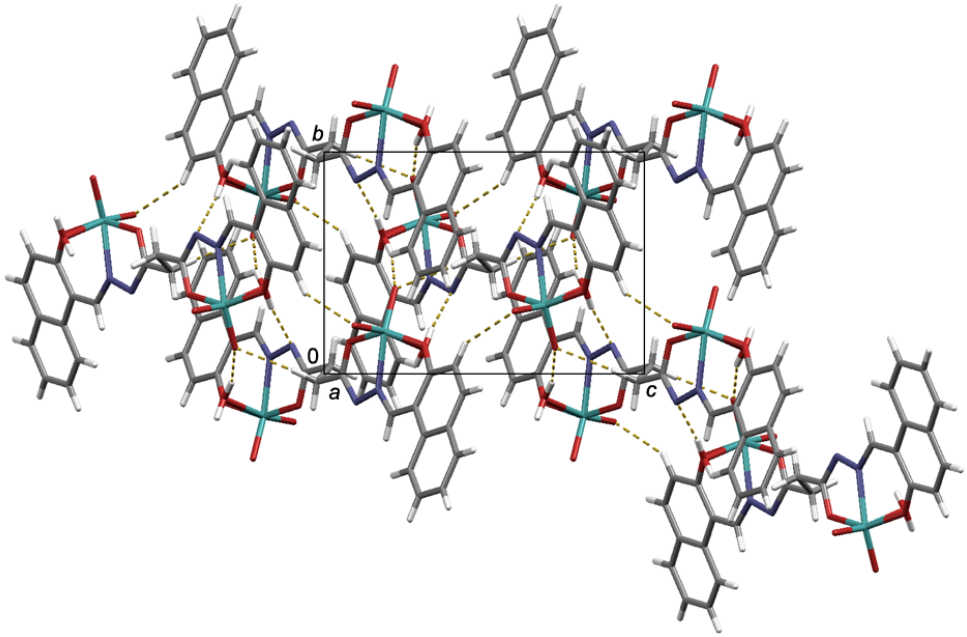

(a)

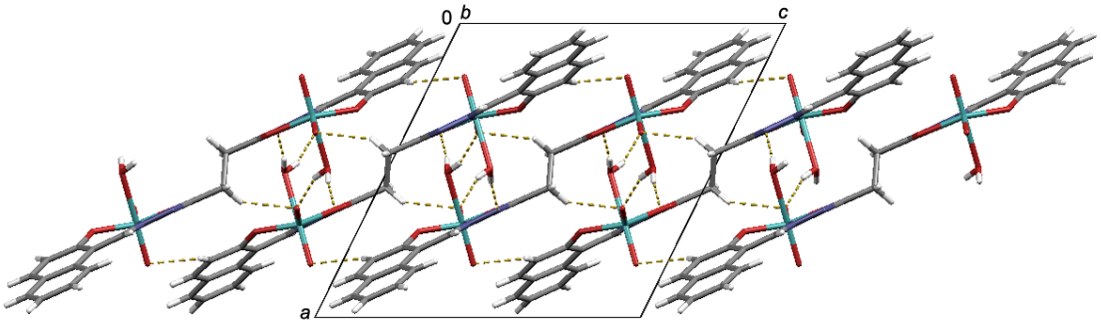

(b)

Figure S6. Fragment of crystal structure in **[$Mo_2O_4(H_2O)_2(L^2)$]** shown down the: (a) *a*-axis, and (b) *b*-axis.

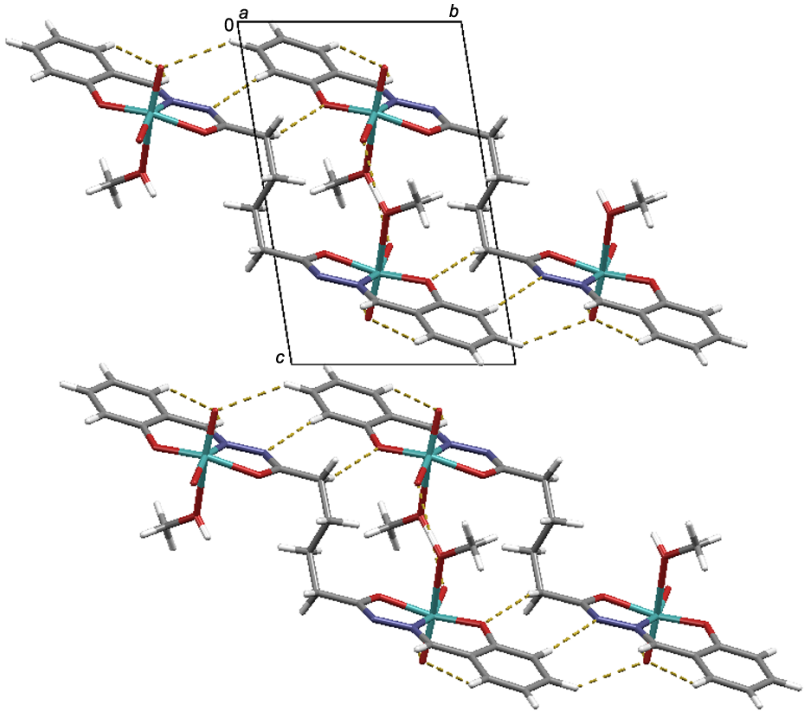

(a)

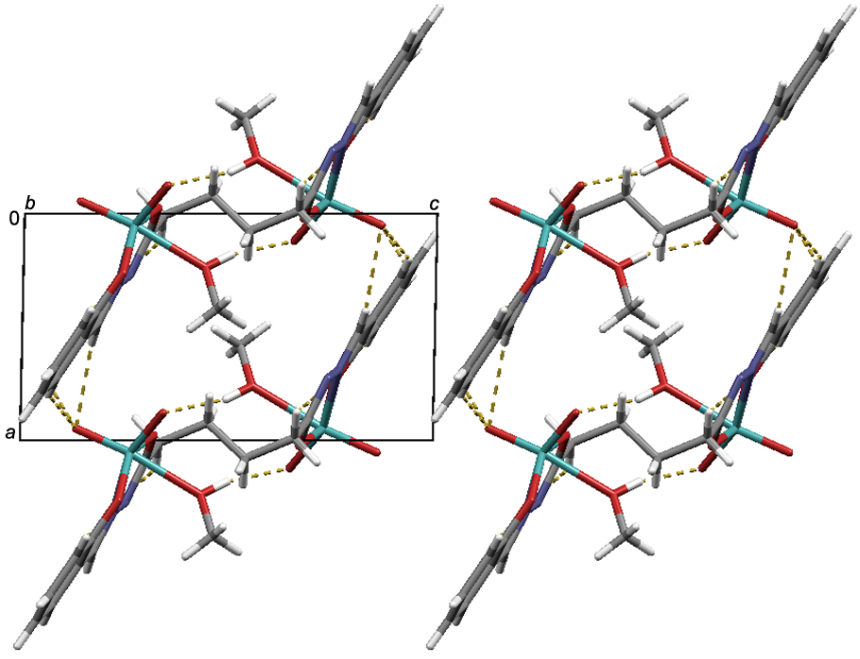

(b)

Figure S7. Fragment of crystal structure in **[$Mo_2O_4(MeOH)_2(L^5)$]** shown down the: (a) *a*-axis, and (b) *b*-axis.

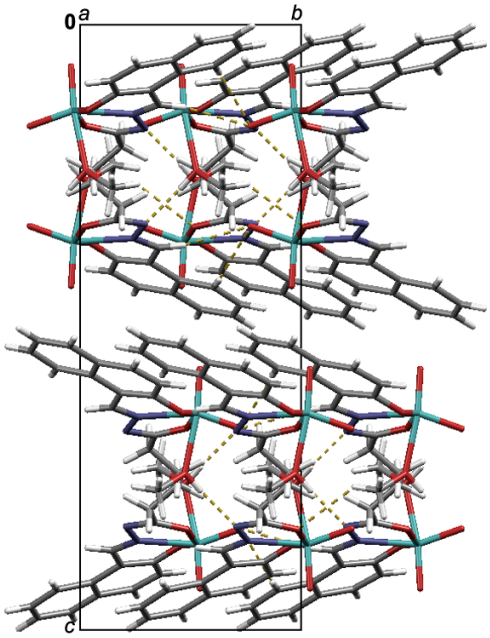

(a)

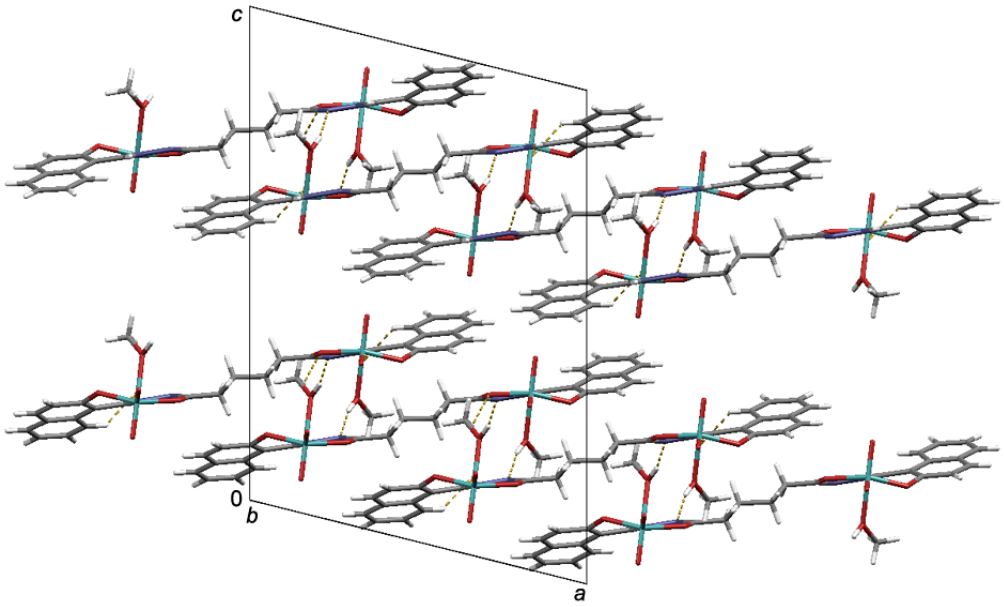

(b)

Figure S8. Fragment of crystal structure in **[$Mo_2O_4(MeOH)_2(L^6)$]** shown down the: (a) *a*-axis, and (b) *b*-axis.

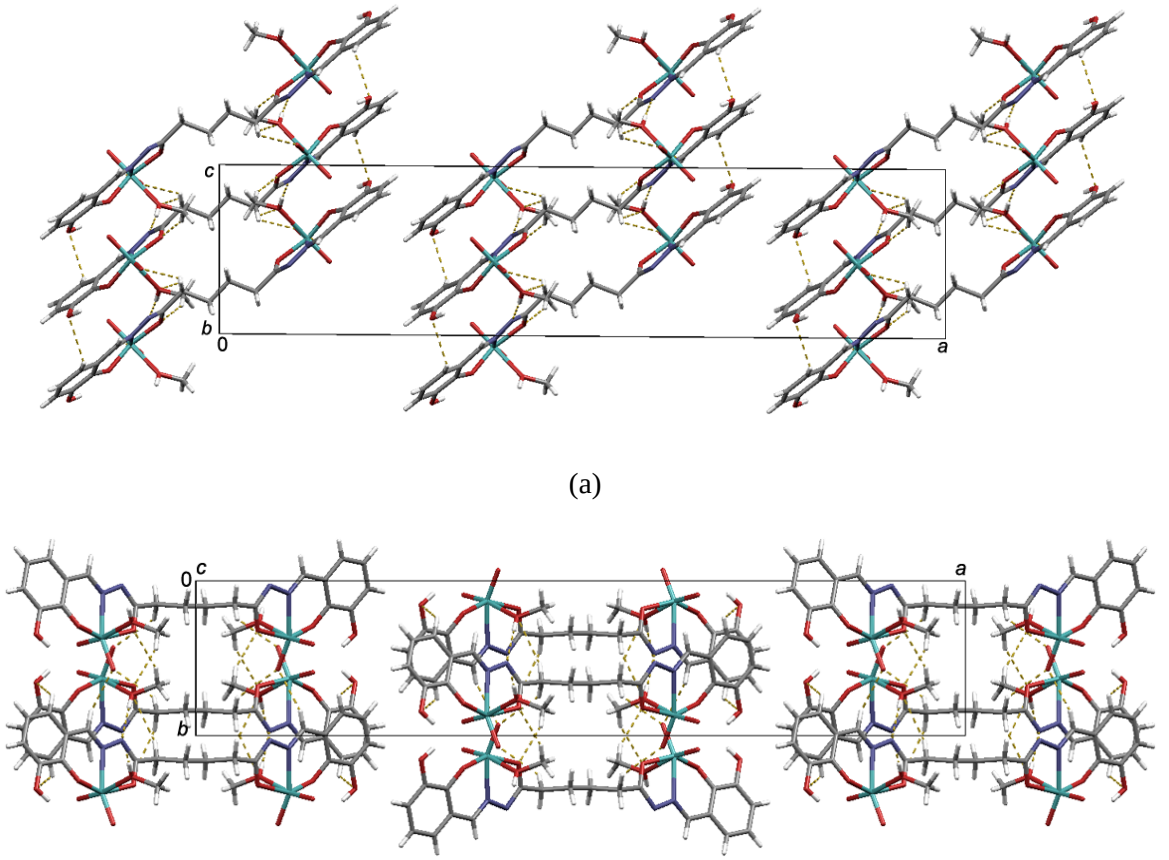

Figure S9. Fragment of crystal structure in **[$Mo_2O_4(MeOH)_2(L^7)$]** shown down the: (a) *b*-axis, and (b) *c*-axis.

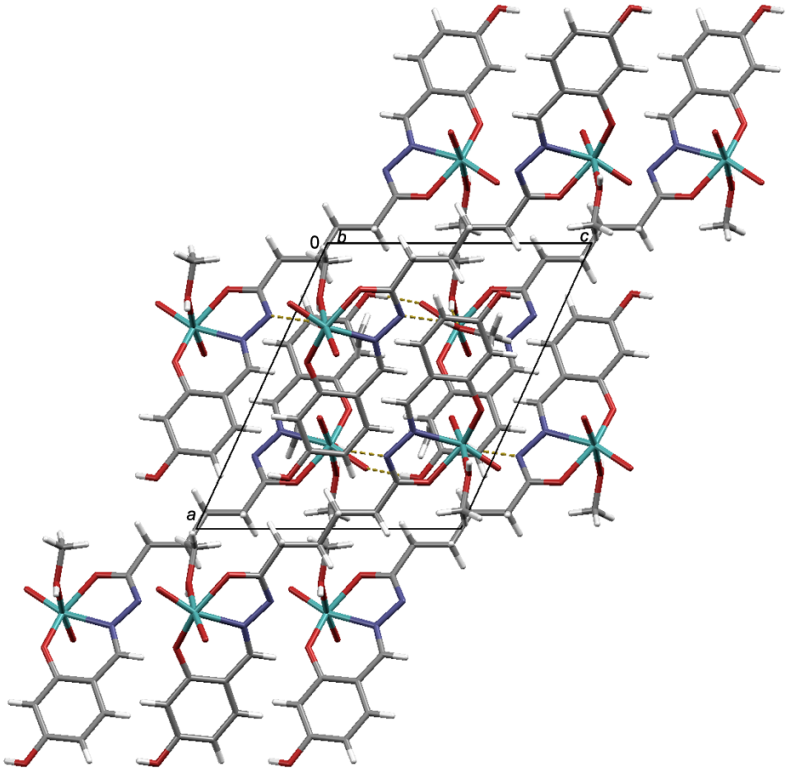

(a)

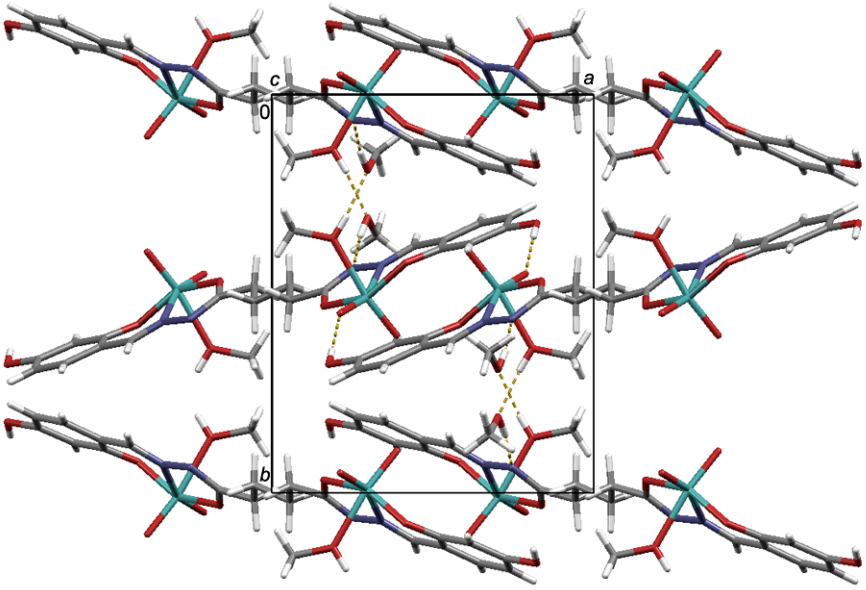

(b)

Figure S10. Fragment of crystal structure in **[$Mo_2O_4(MeOH)_2(L^8)$] 2MeOH** shown down the: (a) *b*-axis, and (b) *c*-axis.

TGA Analysis

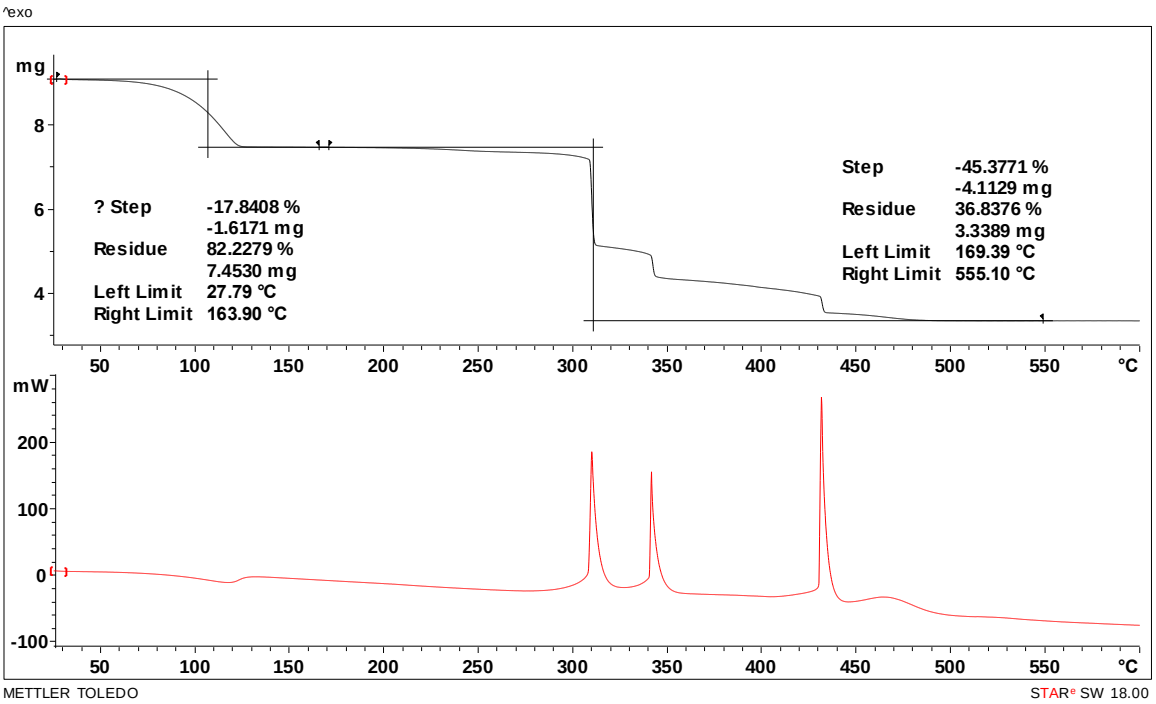

Figure S11. TGA/DSC analysis of **$[Mo_2O_4(MeOH)_2(L^1)]\cdot 2MeOH$.**

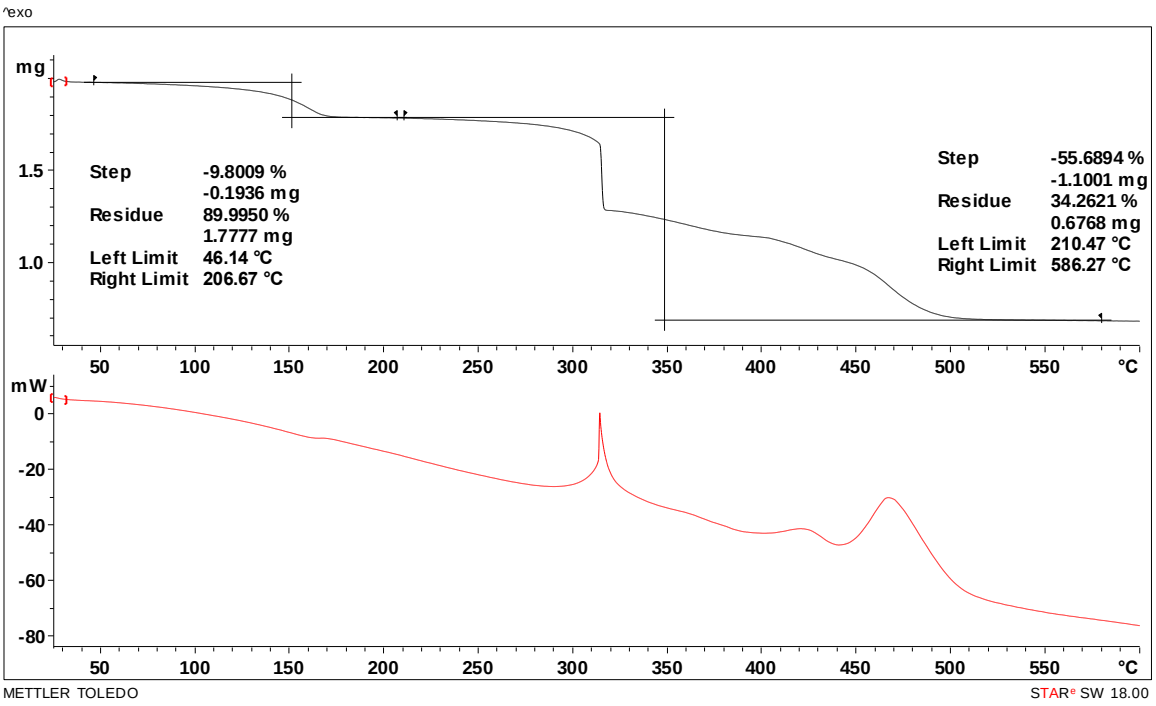

Figure S12. TGA/DSC analysis of **$[Mo_2O_4(MeOH)_2(L^2)]$.**

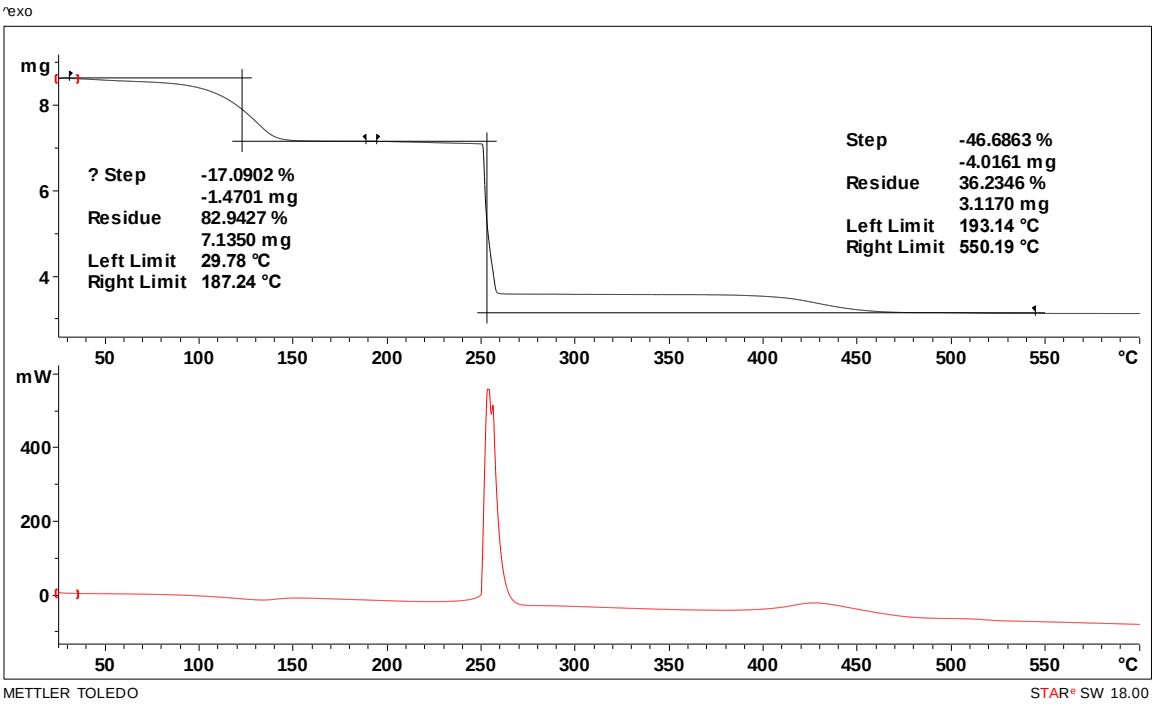

Figure S13. TGA/DSC analysis of **$[Mo_2O_4(MeOH)_2(L^3)]\cdot 2MeOH$.**

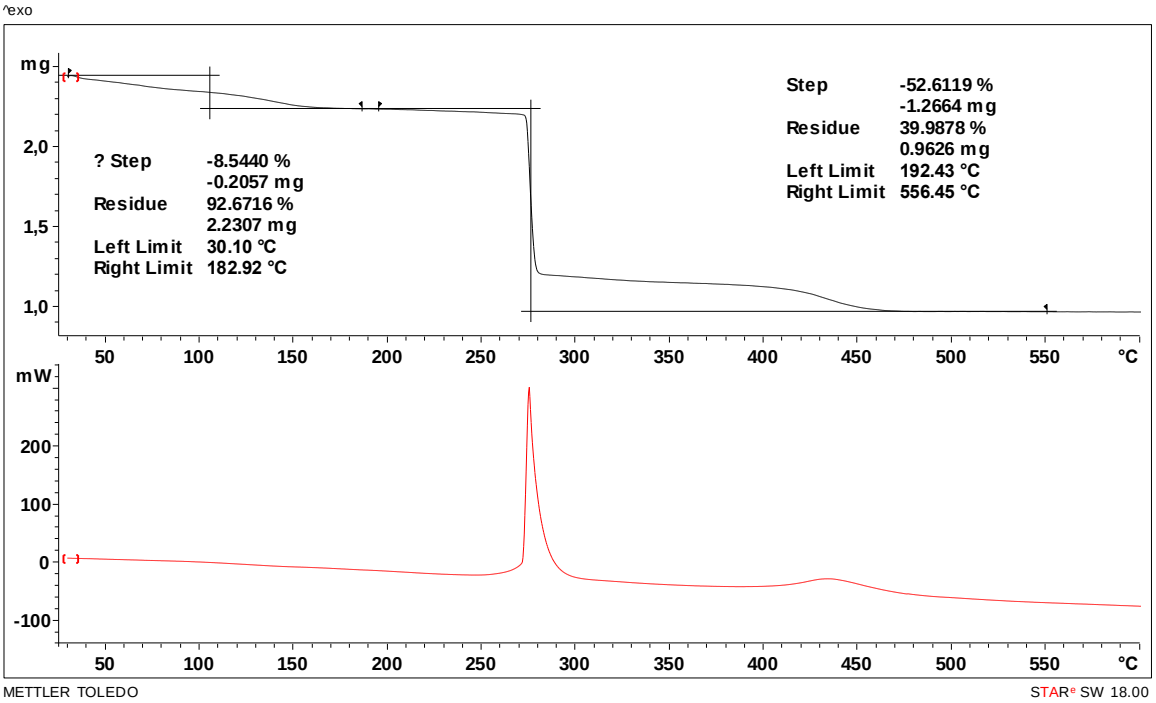

Figure S14. TGA/DSC analysis of **$[Mo_2O_4(MeOH)_2(L^4)]$.**

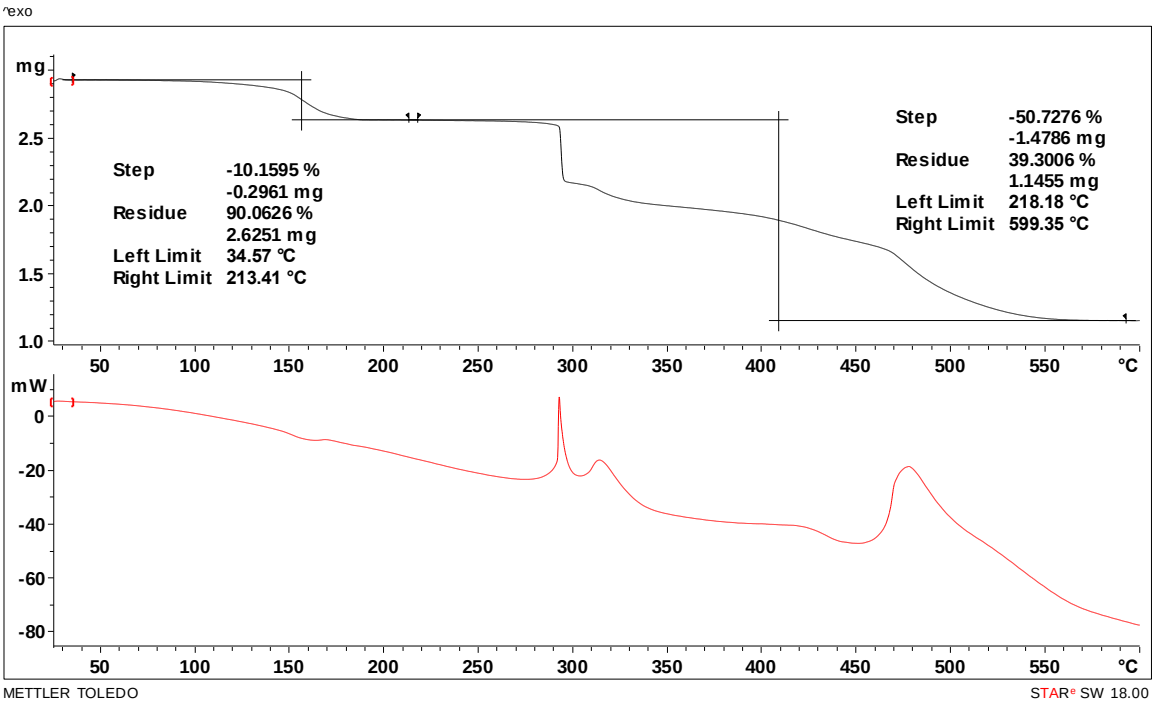

Figure S15. TGA/DSC analysis of **[$Mo_2O_4(MeOH)_2(L^5)$].**

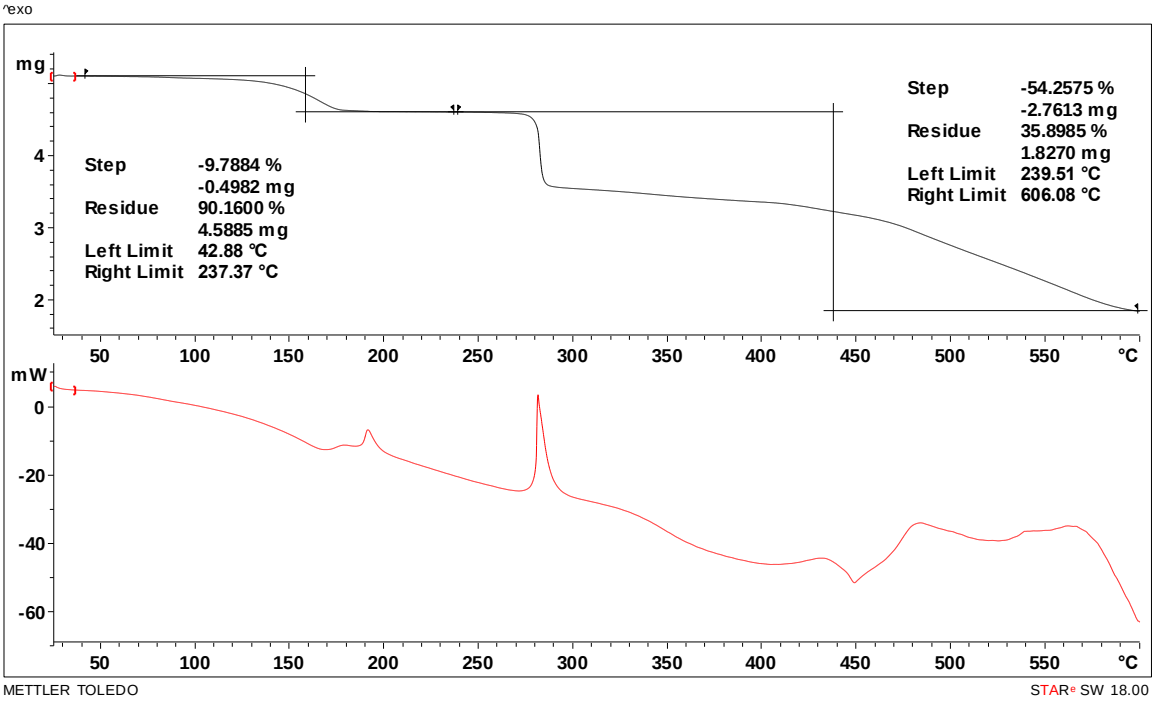

Figure S16. TGA/DSC analysis of **[$Mo_2O_4(MeOH)_2(L^6)$].**

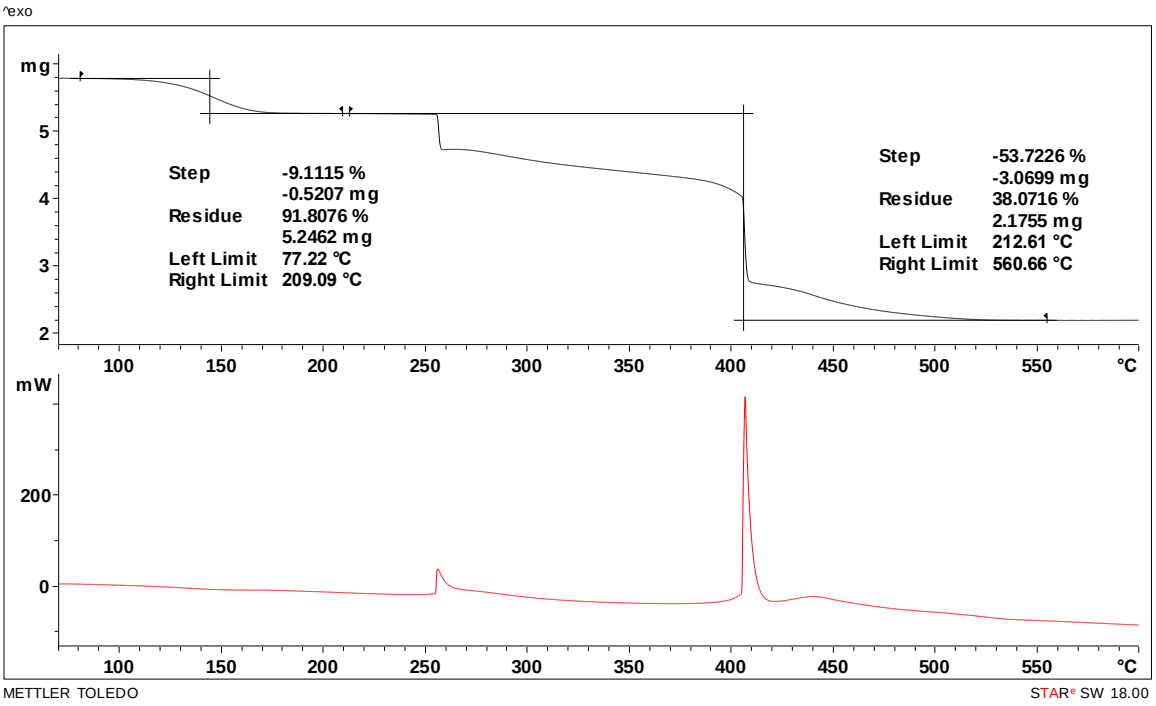

Figure S17. TGA/DSC analysis of **[$Mo_2O_4(MeOH)_2(L^7)$].**

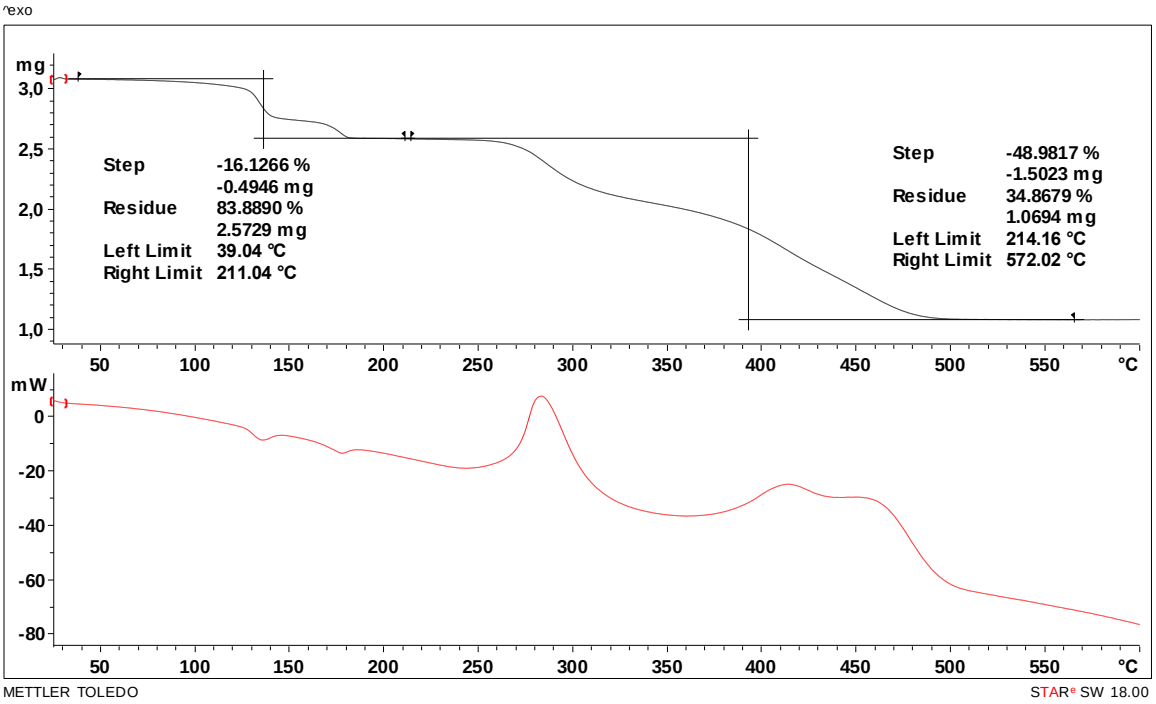

Figure S18. TGA/DSC analysis of **[$Mo_2O_4(MeOH)_2(L^8)$]·2MeOH.**

Powder X-ray diffraction

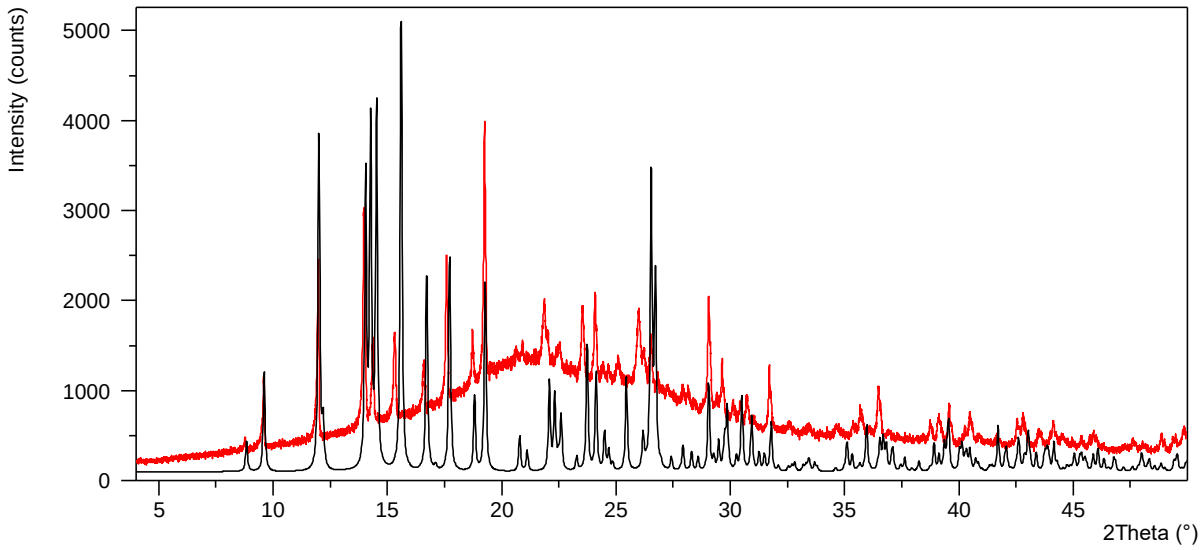

Figure S19. Measured (red) and calculated (black) powder X-ray diffraction pattern of **$[Mo_2O_4(MeOH)_2(L^1)]\cdot 2MeOH$.** The small differences between peak positions and intensities can be attributed to difference in data collection temperature for powder and single-crystal data.

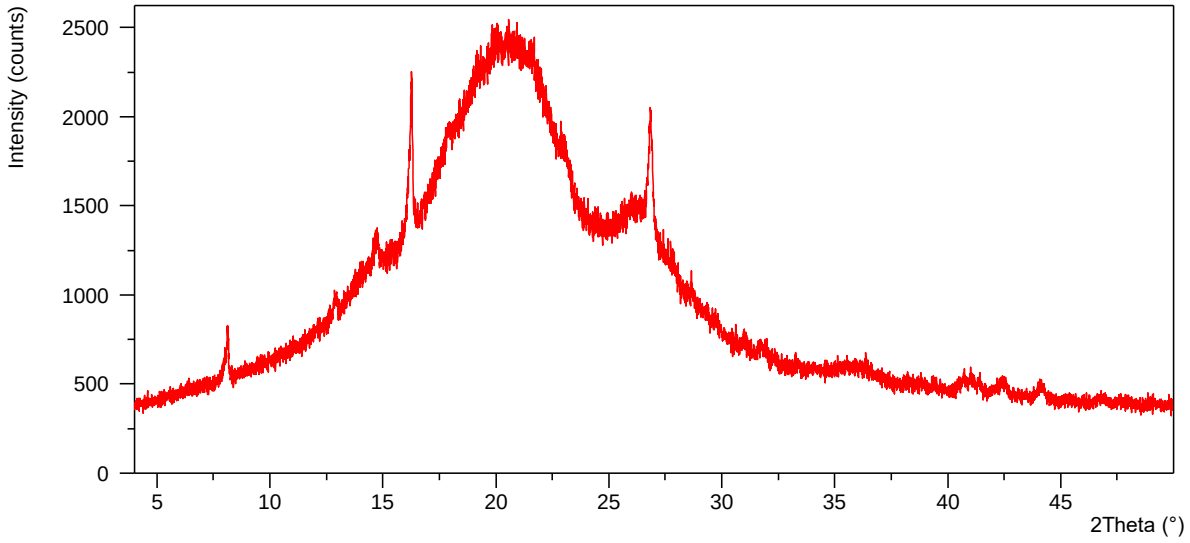

Figure S20. Measured powder X-ray diffraction pattern of **$[Mo_2O_4(MeOH)_2(L^2)]$.** The pattern shows significant contribution from amorphous phase and low crystallinity. As the single crystal differs in coordinated solvent, no attempt in comparison to calculated data was made.

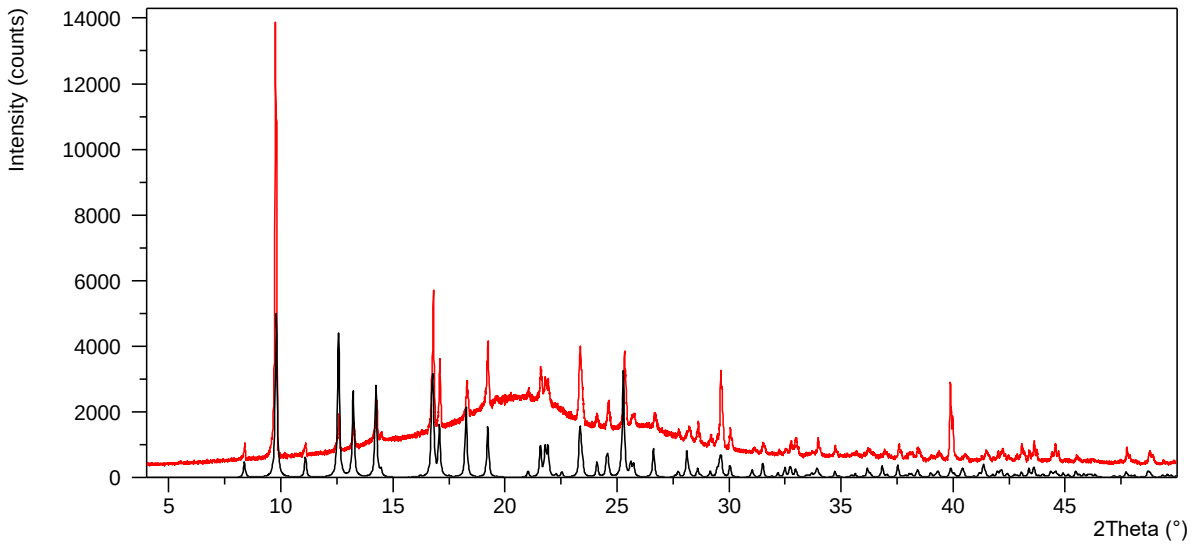

Figure S21. Measured (red) and calculated (black) powder X-ray diffraction pattern of **$[Mo_2O_4(MeOH)_2(L^3)]\cdot 2MeOH$.** The small differences between peak positions and intensities can be attributed to difference in data collection temperature for powder and single-crystal data.

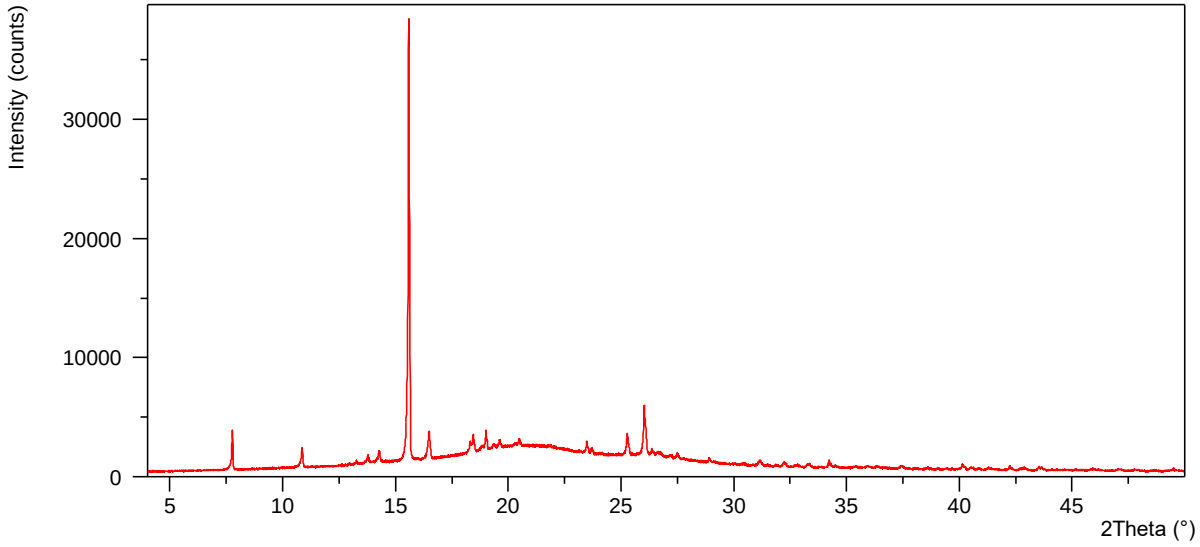

Figure S22. Measured powder X-ray diffraction pattern of **$[Mo_2O_4(MeOH)_2(L^4)]$.** The pattern shows significant contribution from amorphous phase and low crystallinity. As the single crystal contains additional crystal solvent, no attempt in comparison to calculated data was made.

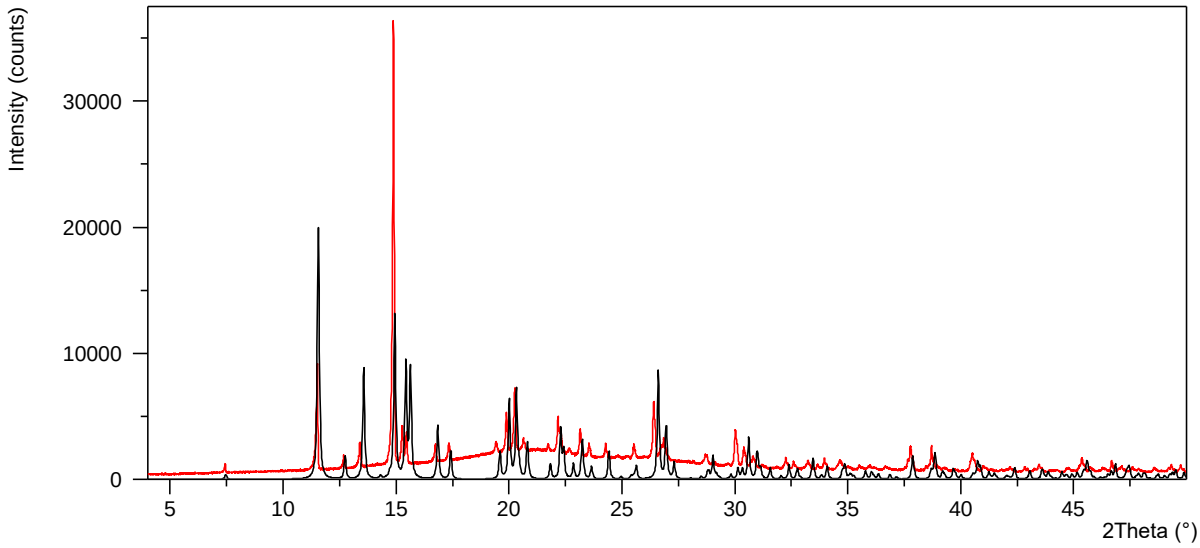

Figure S23. Measured (red) and calculated (black) powder X-ray diffraction pattern of **[$Mo_2O_4(MeOH)_2(L^5)$].** The small differences between peak positions and intensities can be attributed to difference in data collection temperature for powder and single-crystal data.

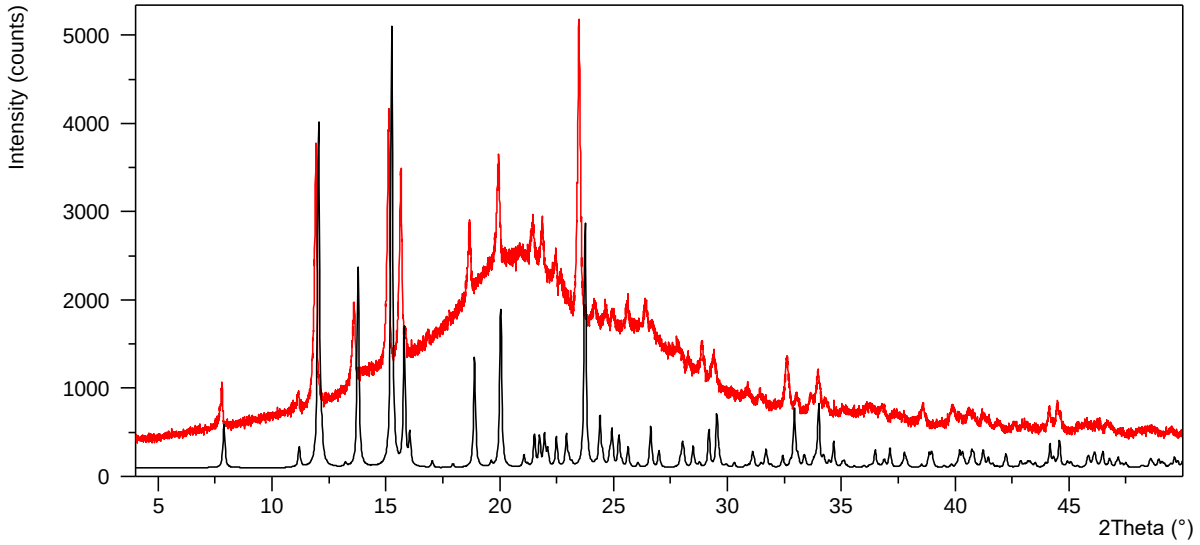

Figure S24. Measured (red) and calculated (black) powder X-ray diffraction pattern of **[$Mo_2O_4(MeOH)_2(L^6)$].** The small differences between peak positions and intensities can be attributed to difference in data collection temperature for powder and single-crystal data.

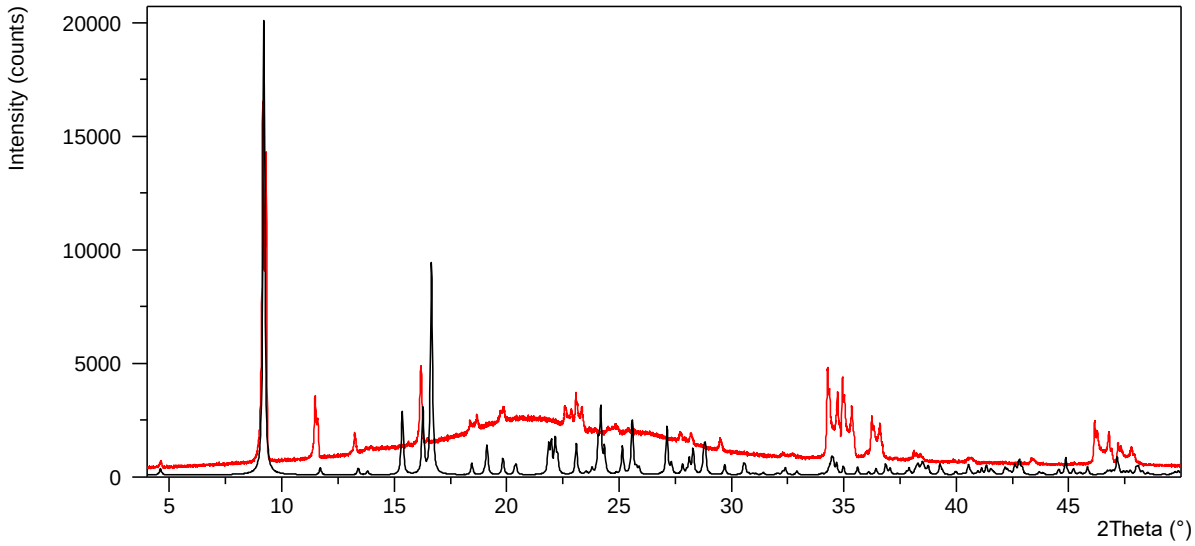

Figure S25. Measured (red) and calculated (black) powder X-ray diffraction pattern of **[$Mo_2O_4(MeOH)_2(L^7)$].** The small differences between peak positions and intensities can be attributed to difference in data collection temperature for powder and single-crystal data.

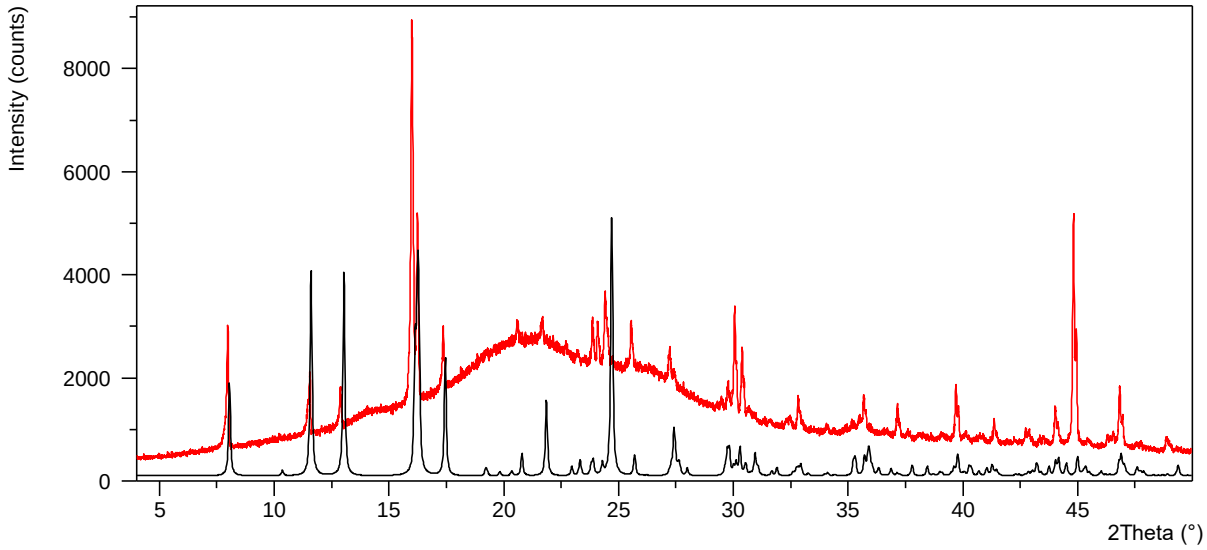

Figure S26. Measured (red) and calculated (black) powder X-ray diffraction pattern of **[$Mo_2O_4(MeOH)_2(L^8)$]·2MeOH.** The small differences between peak positions and intensities can be attributed to difference in data collection temperature for powder and single-crystal data.

NMR spectroscopy

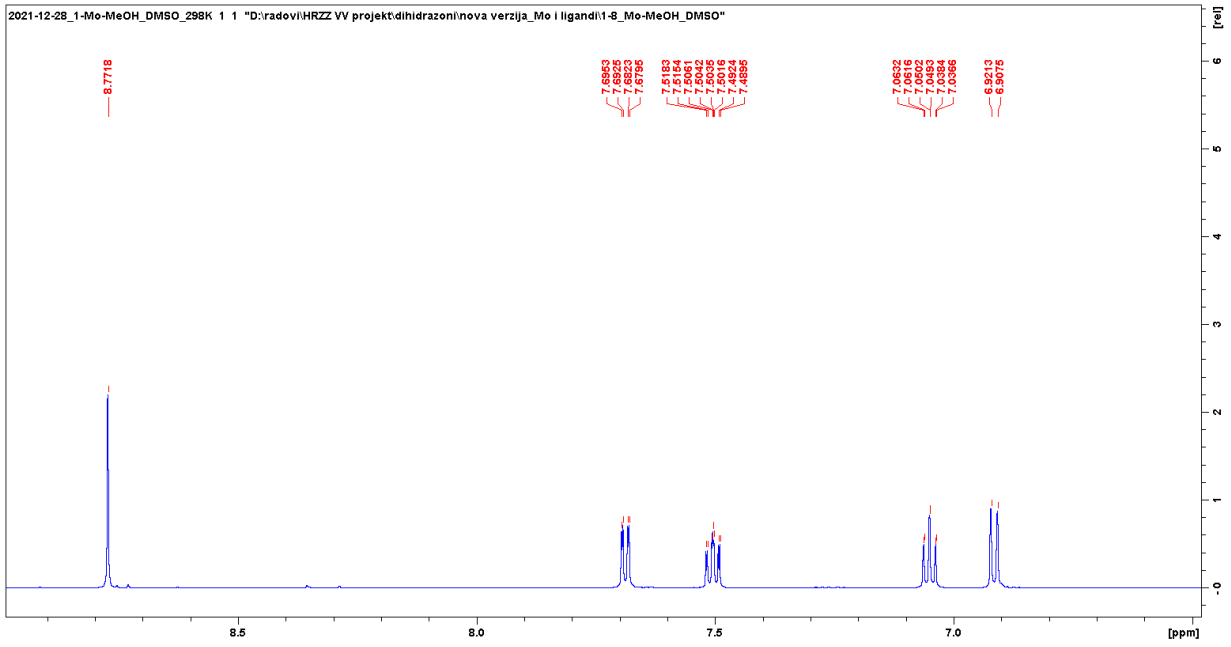

(a)

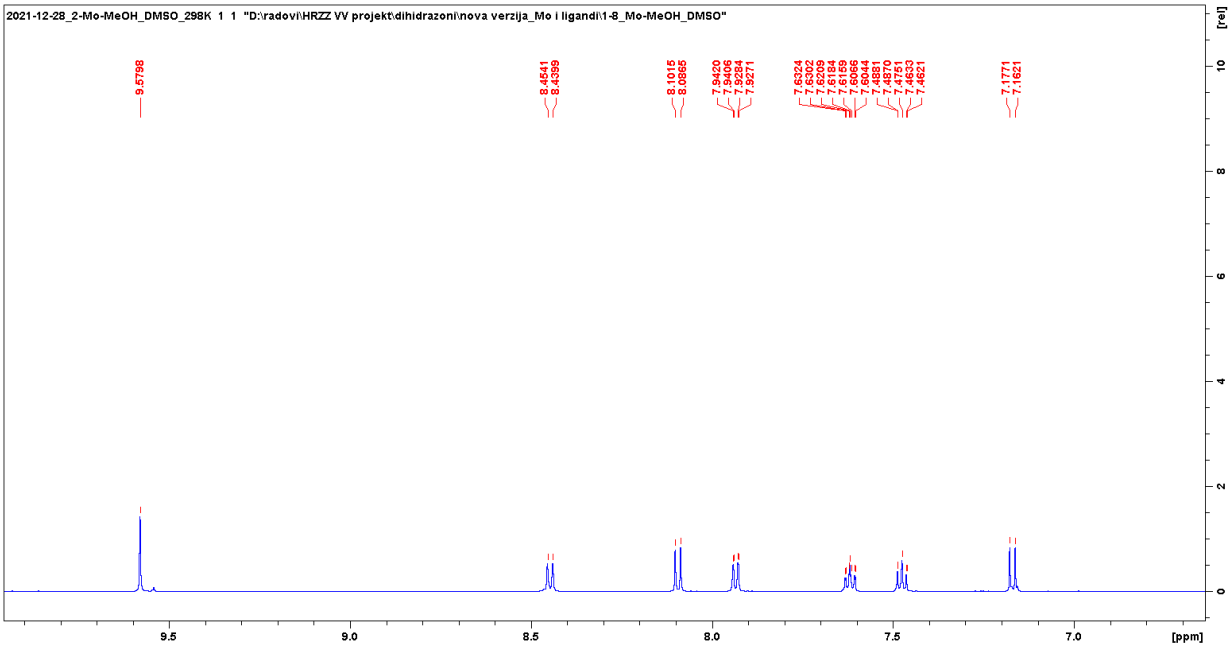

(b)

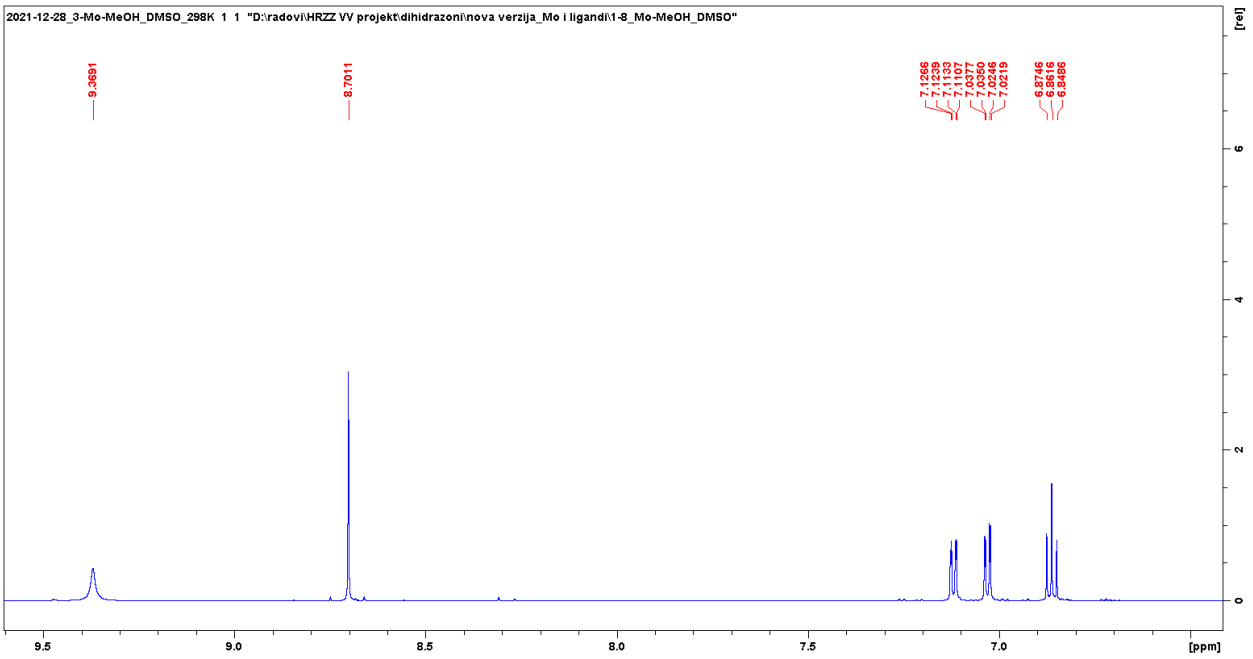

(c)

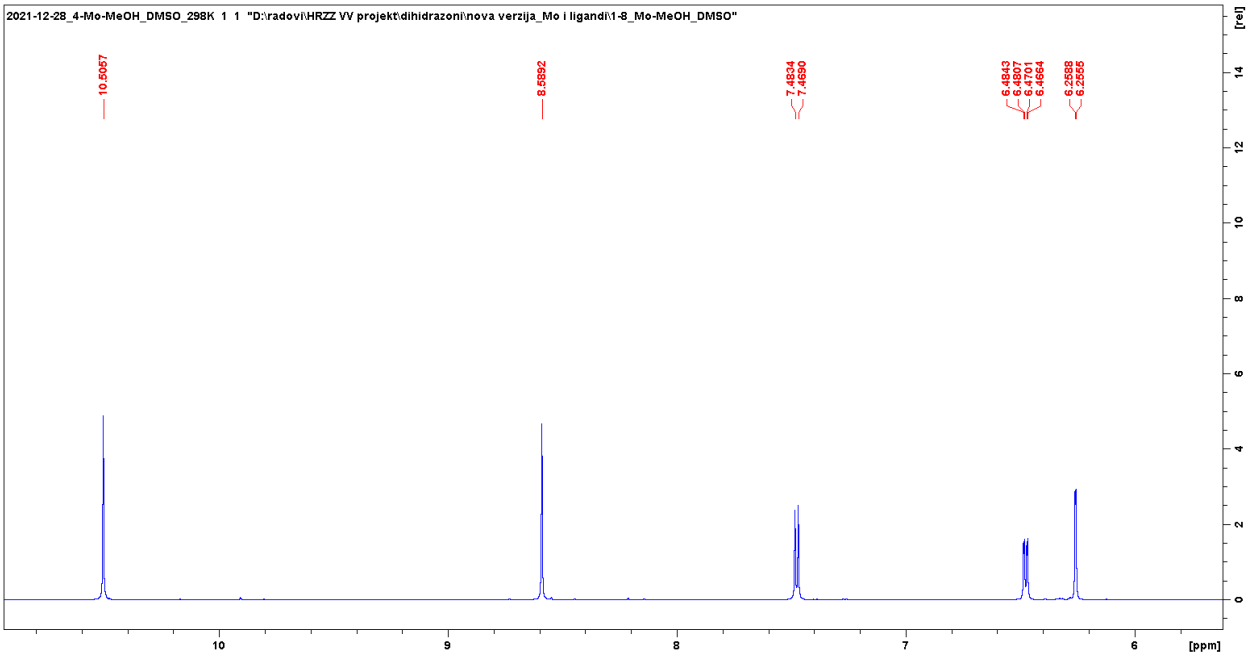

(d)

Figure S27. ^{1}H NMR spectra in selected region for succinyl-type of complexes: (a) **[$Mo_2O_4(MeOH)_2(L^1)$];** **(b) [$Mo_2O_4(MeOH)_2(L^2)$]**; (c) **[$Mo_2O_4(MeOH)_2(L^3)$]**; (d) **[$Mo_2O_4(MeOH)_2(L^4)$]** in DMSO–d_6 at 298 K

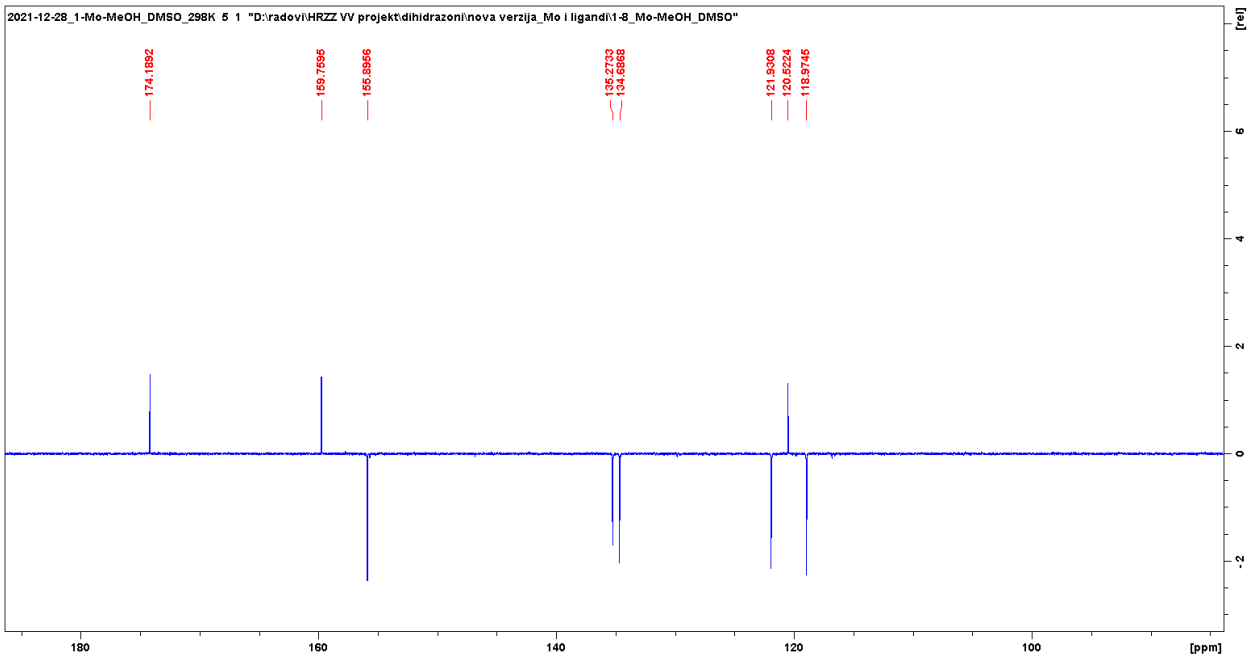
2021-12-28_1-Mo-MeOH_DMSO_298K 5 1 "D:\radovi\HRZZ VV projekt\dihidrazoni\nova verzija_Mo i ligandi\1-8_Mo-MeOH_DMSO"
174.1892
159.7595
155.8966
135.2733
134.6868
121.9308
120.5224
118.9745
[rel]
6
4
2
0
-2
180
160
140
120
100
[ppm]

(a)

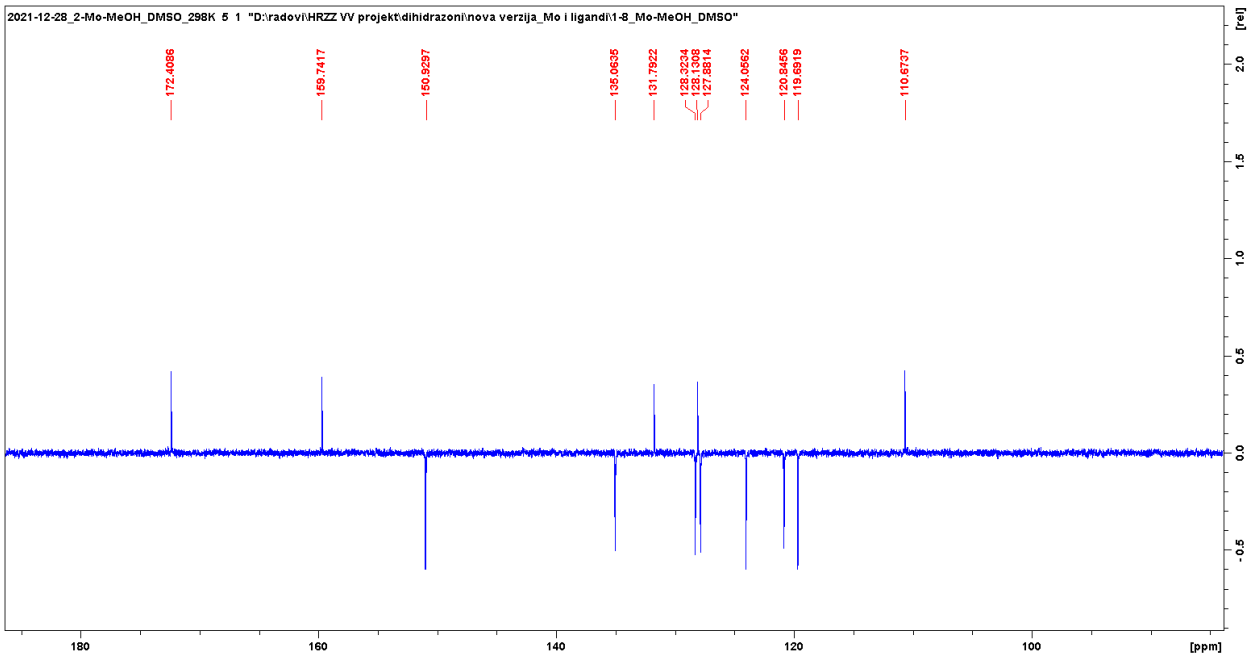
2021-12-28_2-Mo-MeOH_DMSO_298K 5 1 "D:\radovi\HRZZ VV projekt\dihidrazoni\nova verzija_Mo i ligandi\1-8_Mo-MeOH_DMSO"
172.4086
159.7417
150.9257
135.0635
131.7922
128.3234
128.1308
127.8814
124.0562
120.8456
119.6919
110.6737
[rel]
2.0
1.5
1.0
0.5
0.0
-0.5
180
160
140
120
100
[ppm]

(b)

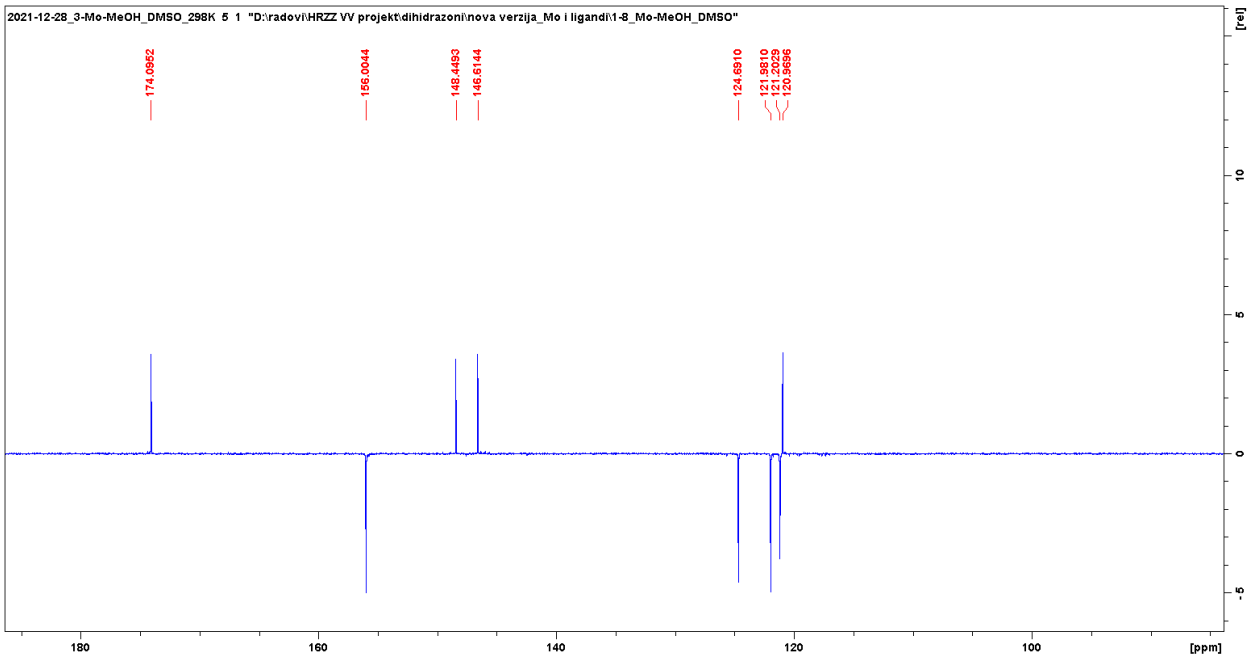

(c)

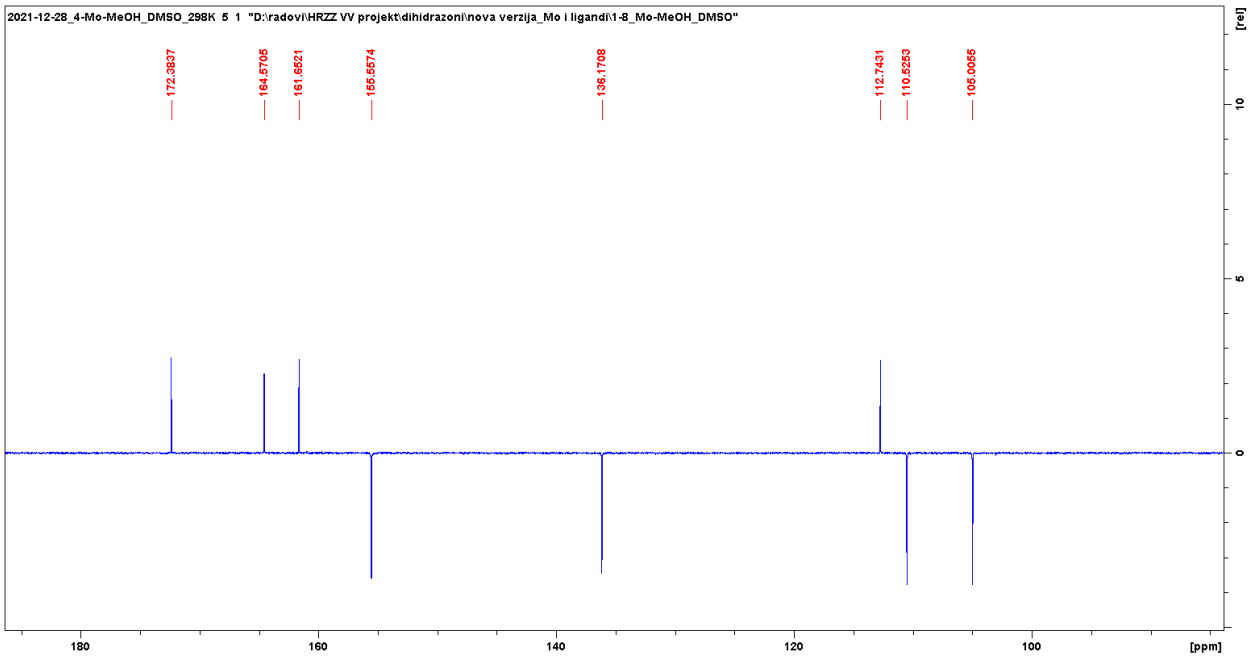

(d)

Figure S28. ^{13}C NMR spectra in selected region for succinyl-type of complexes: (a) **[$Mo_2O_4(MeOH)_2(L^1)$]; (b) [$Mo_2O_4(MeOH)_2(L^2)$]**; (c) **[$Mo_2O_4(MeOH)_2(L^3)$]**; (d) **[$Mo_2O_4(MeOH)_2(L^4)$]** in DMSO–d_6 at 298 K.

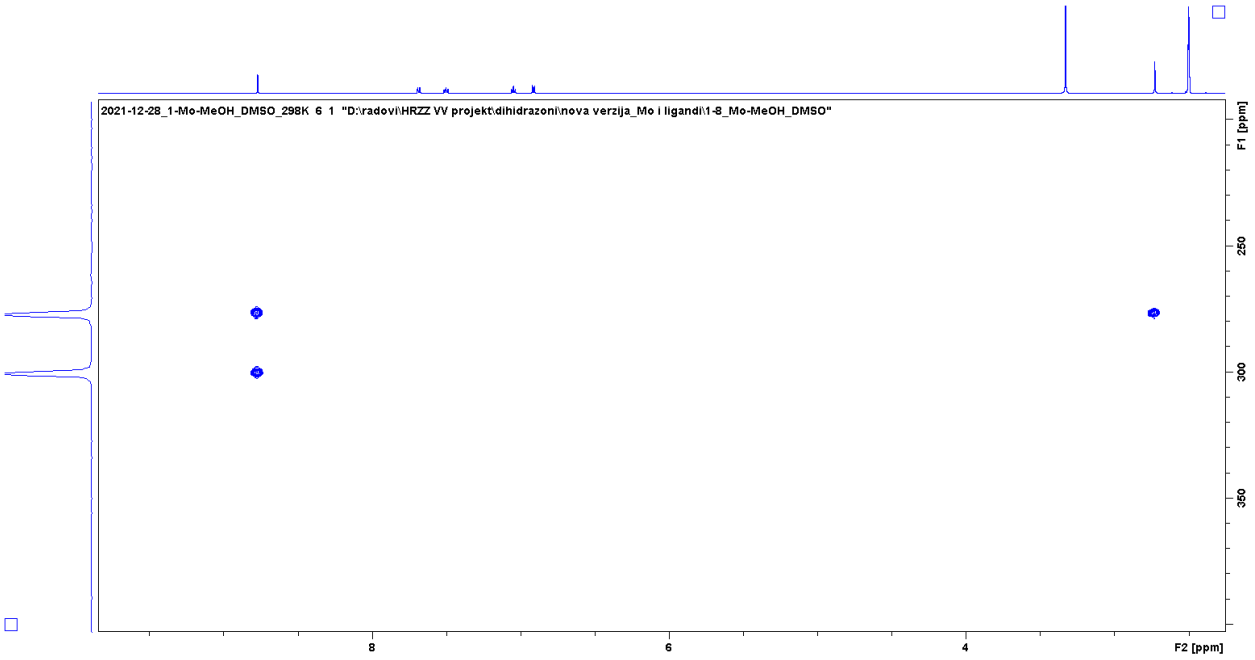
2021-12-28_1-Mo-MeOH_DMSO_298K 6 1 "D:\radovi\HRZZ VV projekt\dihidrazoni\nova verzija_Mo i ligandi\1-8_Mo-MeOH_DMSO"
F1 [ppm]
250
300
350
8
6
4
F2 [ppm]

(a)

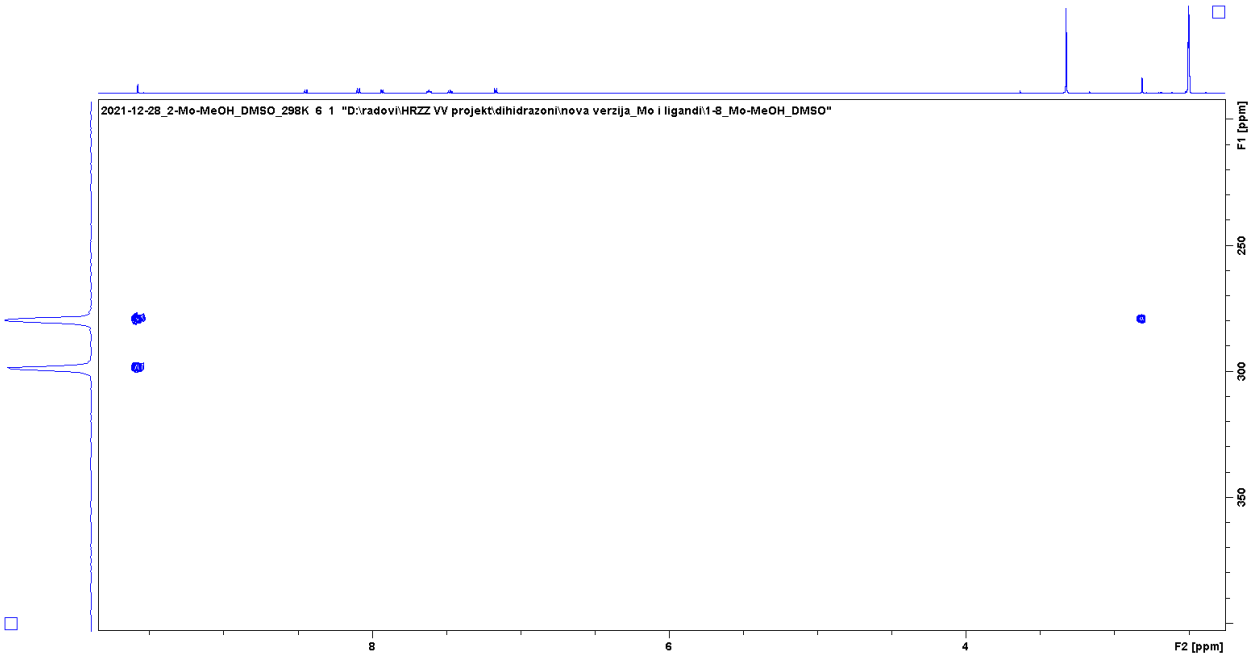
2021-12-28_2-Mo-MeOH_DMSO_298K 6 1 "D:\radovi\HRZZ VV projekt\dihidrazoni\nova verzija_Mo i ligandi\1-8_Mo-MeOH_DMSO"
F1 [ppm]
250
300
350
8
6
4
F2 [ppm]

(b)

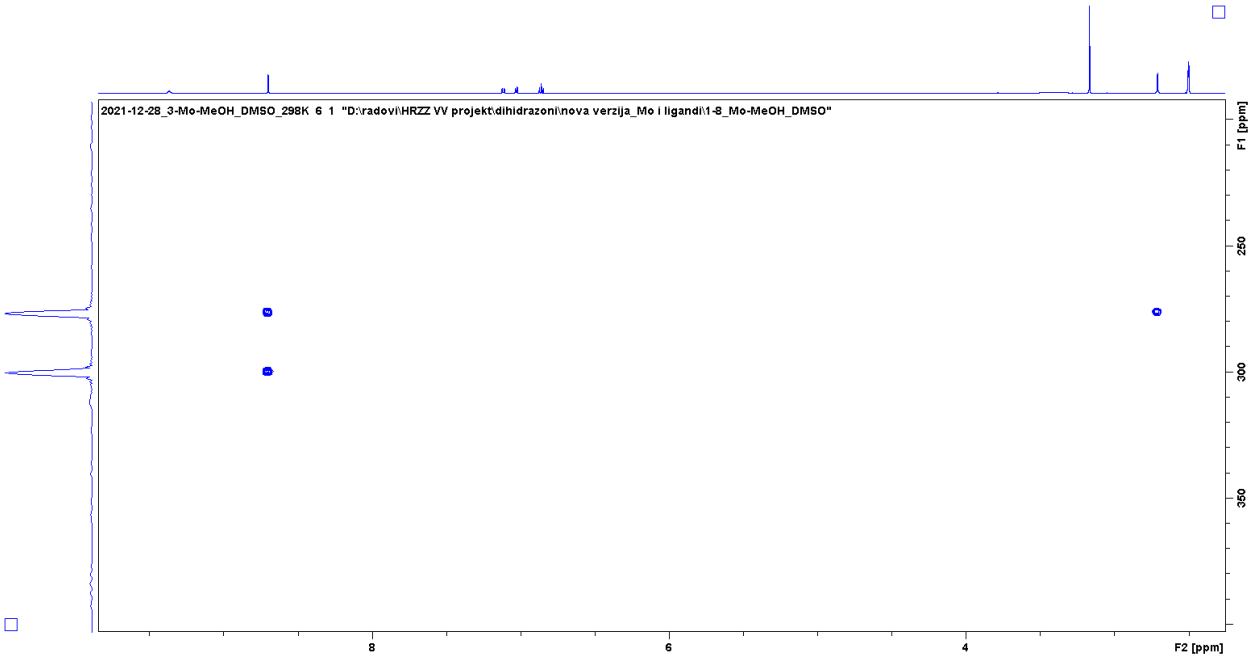

(c)

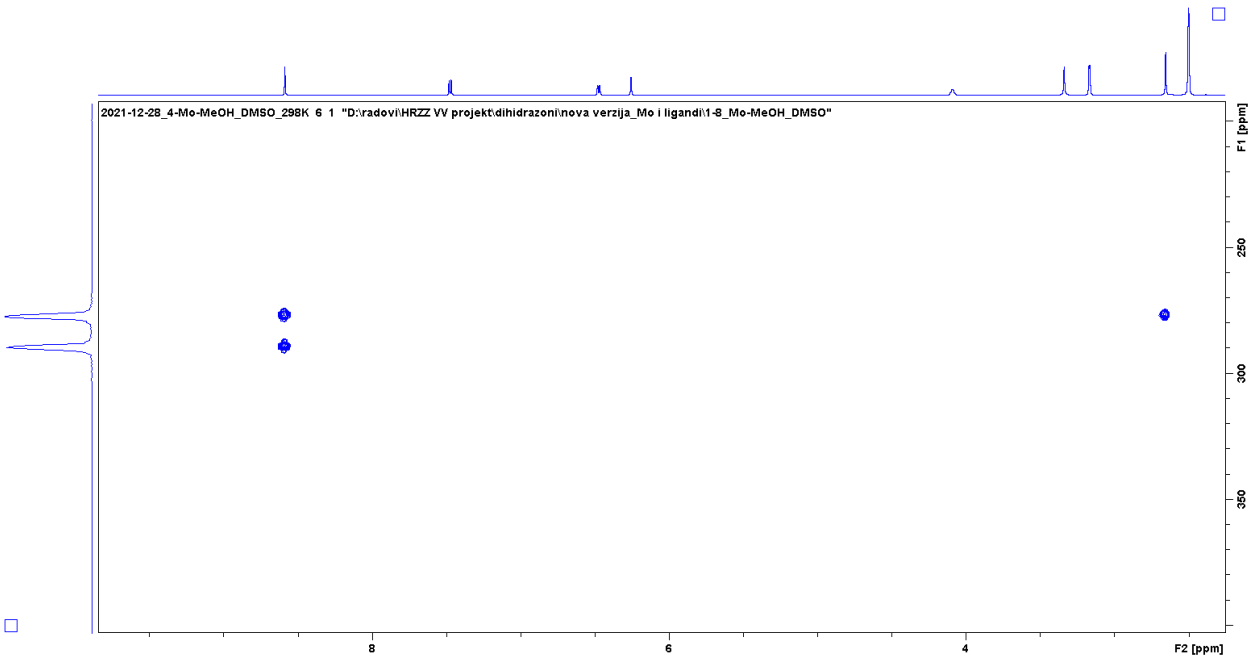

(d)

Figure S29. ^{1}H-^{15}N HMBC NMR spectra in selected region for succinyl-type of complexes: (a) **[$Mo_2O_4(MeOH)_2(L^1)$]; (b) [$Mo_2O_4(MeOH)_2(L^2)$]**; (c) **[$Mo_2O_4(MeOH)_2(L^3)$]**; (d) **[$Mo_2O_4(MeOH)_2(L^4)$]** in DMSO–d_6 at 298 K.

Table S8. ^{1}H, ^{13}C and ^{15}N chemical shifts for succinyl-type of complexes (**$[Mo_2O_4(MeOH)_2(L^1\text{-}L^4)]$**) in DMSO–$d_6$ at 298 K, with the atom numbering scheme

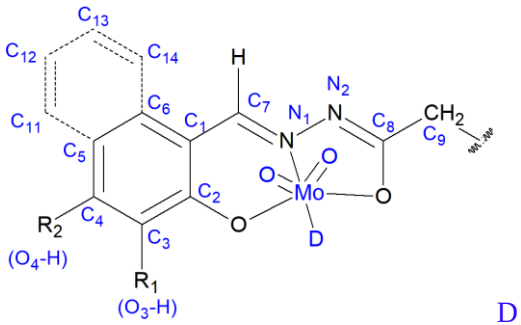

D = MeOH/H_2O/DMSO

	$[Mo_2O_4(MeOH)_2(L^1)]$			**$[Mo_2O_4(MeOH)_2(L^2)]$**			**$[Mo_2O_4(MeOH)_2(L^3)]$**			**$[Mo_2O_4(MeOH)_2(L^4)]$**		
atom(s)	$\delta(^1H)$	$\delta(^{13}C)$	$\delta(^{15}N)$	$\delta(^1H)$	$\delta(^{13}C)$	$\delta(^{15}N)$	$\delta(^1H)$	$\delta(^{13}C)$	$\delta(^{15}N)$	$\delta(^1H)$	$\delta(^{13}C)$	$\delta(^{15}N)$
1		120.5			128.1			121.0			112.7	
2		159.8			159.8			148.5			161.7	
3	6.92	119.0		7.17	119.7			146.6		6.26	105.0	
4	7.50	135.3		8.10	135.1		7.03	121.2			164.6	
5	7.05	121.9			110.7		6.86	122.0		6.48	110.5	
6	7.69	134.7			131.8		7.12	124.7		7.48	136.2	
7	8.77	155.9		9.58	150.9		8.70	156.0		8.59	155.6	
8		174.2			172.4			174.1			172.4	
9	2.73	28.0			27.0		2.71	28.2		2.66	27.9	
11				7.94	128.3							
12				7.48	124.1							
13				7.62	127.9							
14				8.45	120.9							
N1			300.1			297.3			299.1			289.1
N2			276.3			279.1			276.3			276.3
O3–H							9.37					
O4–H										10.51		

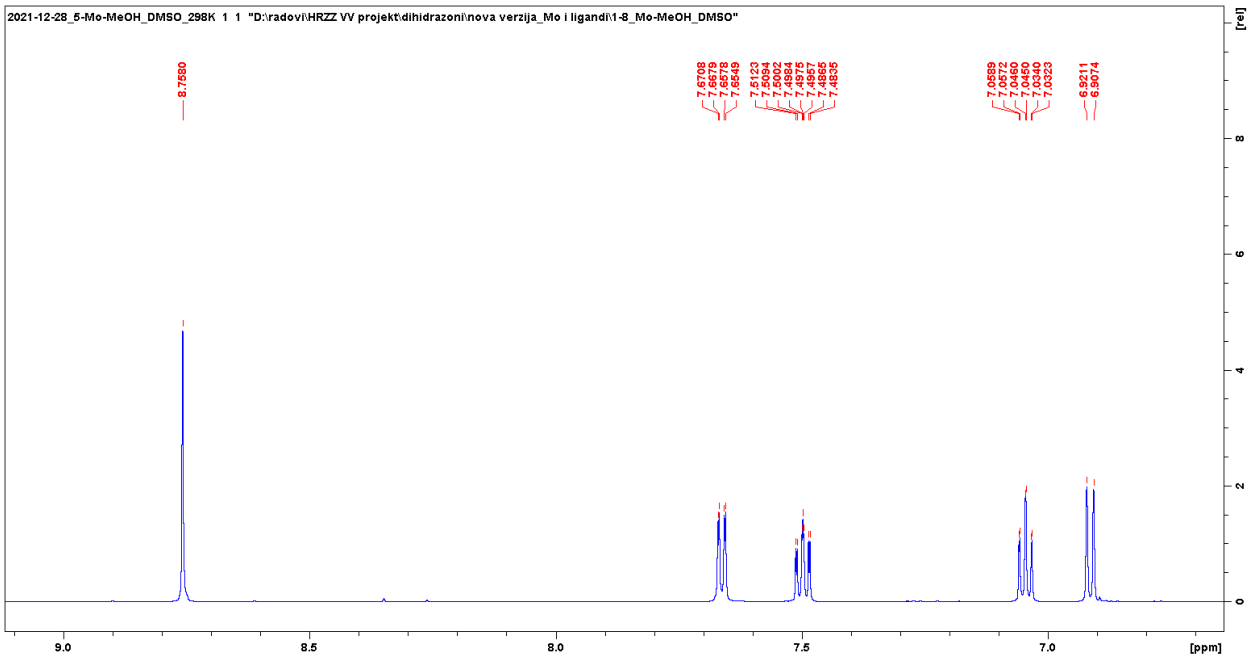
2021-12-28_5-Mo-MeOH_DMSO_298K 1 1 "D:\radovi\HRZZ VV projekt\dihidrazoni\nova verzija_Mo i ligandi\1-8_Mo-MeOH_DMSO"
8.7680
7.6708
7.6679
7.6578
7.6549
7.5123
7.5094
7.5002
7.4984
7.4975
7.4957
7.4885
7.4835
7.0589
7.0572
7.0466
7.0450
7.0340
7.0323
6.9211
6.9074
[rel]
[ppm]

(a)

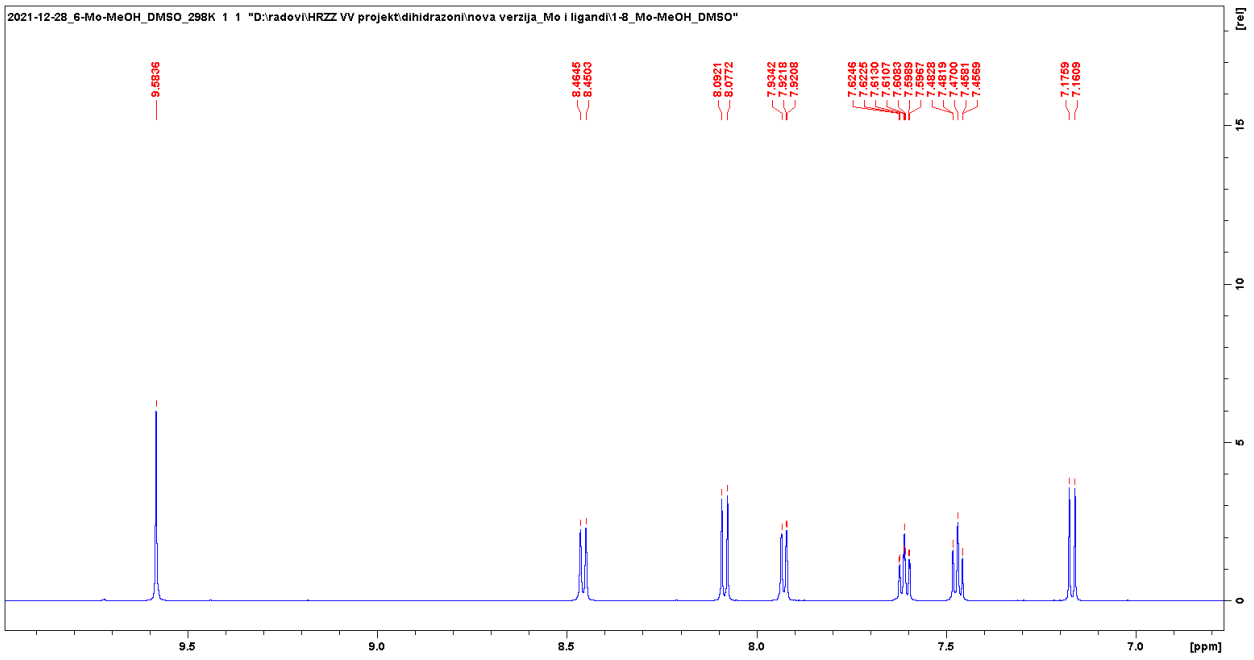
2021-12-28_6-Mo-MeOH_DMSO_298K 1 1 "D:\radovi\HRZZ VV projekt\dihidrazoni\nova verzija_Mo i ligandi\1-8_Mo-MeOH_DMSO"
9.5836
8.4645
8.4503
8.0921
8.0772
7.9342
7.9218
7.9208
7.6246
7.6225
7.6130
7.6107
7.6083
7.5989
7.5957
7.4818
7.4813
7.4700
7.4681
7.4569
7.1759
7.1609
[rel]
[ppm]

(b)

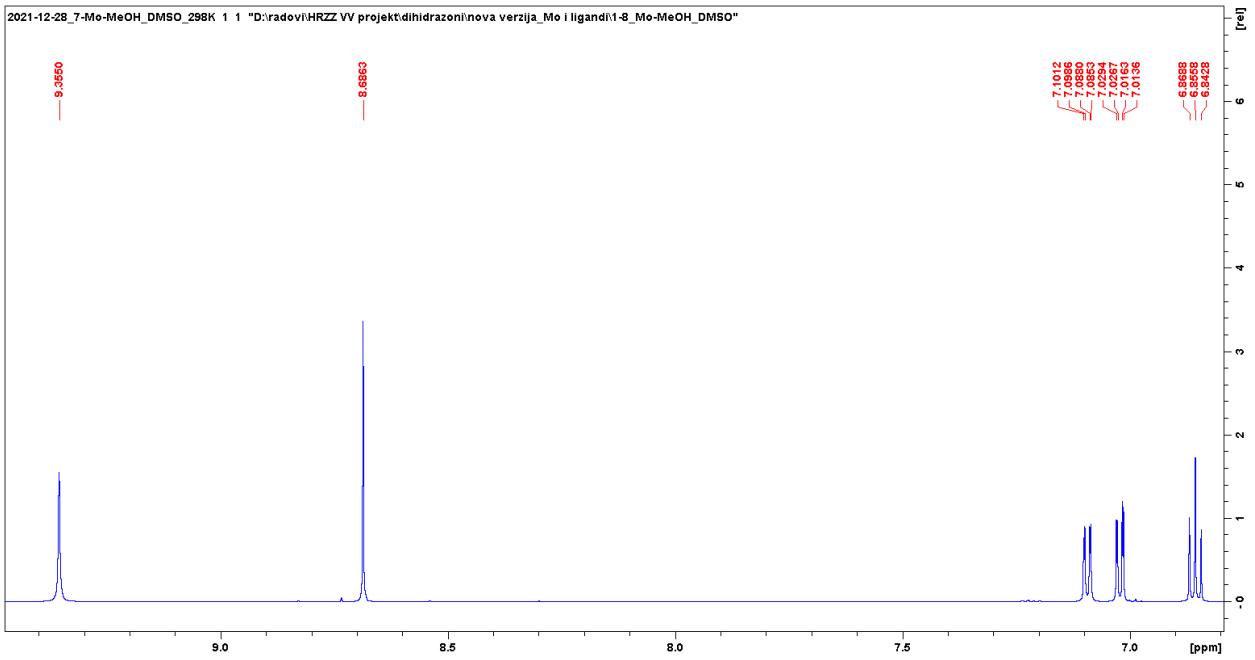

(c)

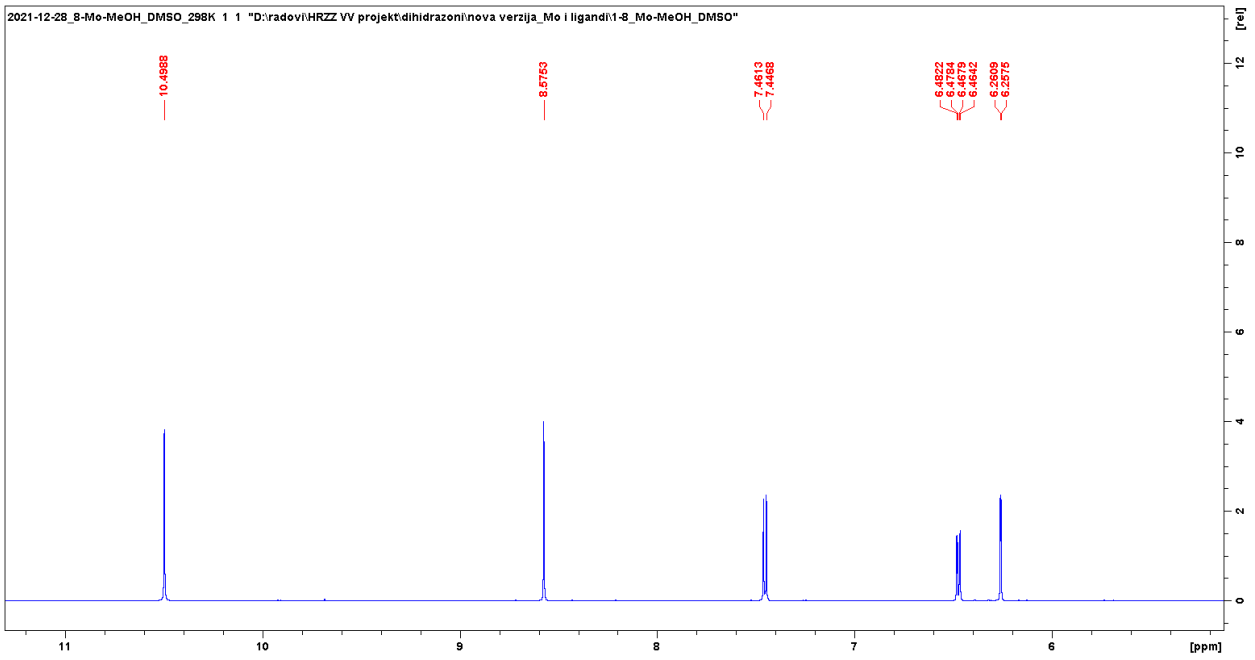

(d)

Figure S30. ^{1}H NMR spectra in selected region for adipoyl-type of complexes: (a) **[$Mo_2O_4(MeOH)_2(L^5)$];** **(b) [$Mo_2O_4(MeOH)_2(L^6)$]**; (c) **[$Mo_2O_4(MeOH)_2(L^7)$]**; (d) **[$Mo_2O_4(MeOH)_2(L^8)$]** in DMSO–d_6 at 298 K.

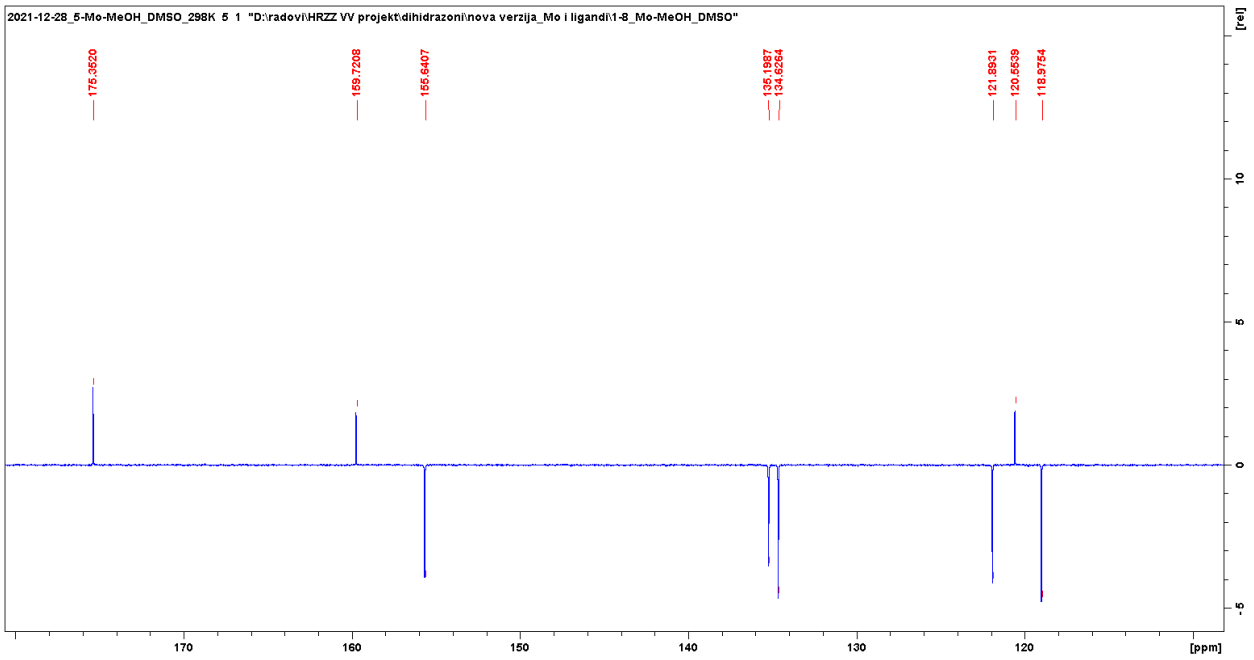
2021-12-28_5-Mo-MeOH_DMSO_298K 5 1 "D:\radovi\HRZZ VV projekt\dihidrazoni\nova verzija_Mo i ligandi\1-8_Mo-MeOH_DMSO"
175.3520
159.7208
155.6407
135.1987
134.6264
121.8931
120.5539
118.9754
[rel]
10
5
0
-5
170
160
150
140
130
120
[ppm]

(a)

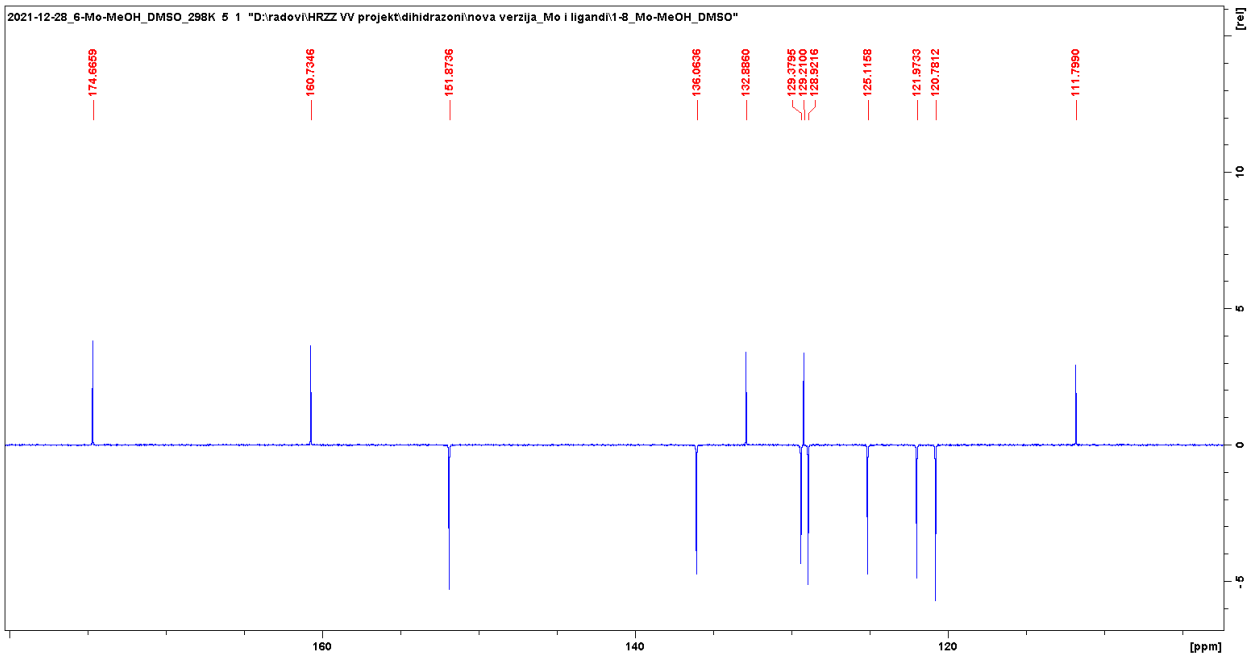
2021-12-28_6-Mo-MeOH_DMSO_298K 5 1 "D:\radovi\HRZZ VV projekt\dihidrazoni\nova verzija_Mo i ligandi\1-8_Mo-MeOH_DMSO"
174.6659
160.7346
151.8736
136.0636
132.8860
129.3795
129.2100
128.9216
125.1158
121.9733
120.7812
111.7990
[rel]
10
5
0
-5
160
140
120
[ppm]

(b)

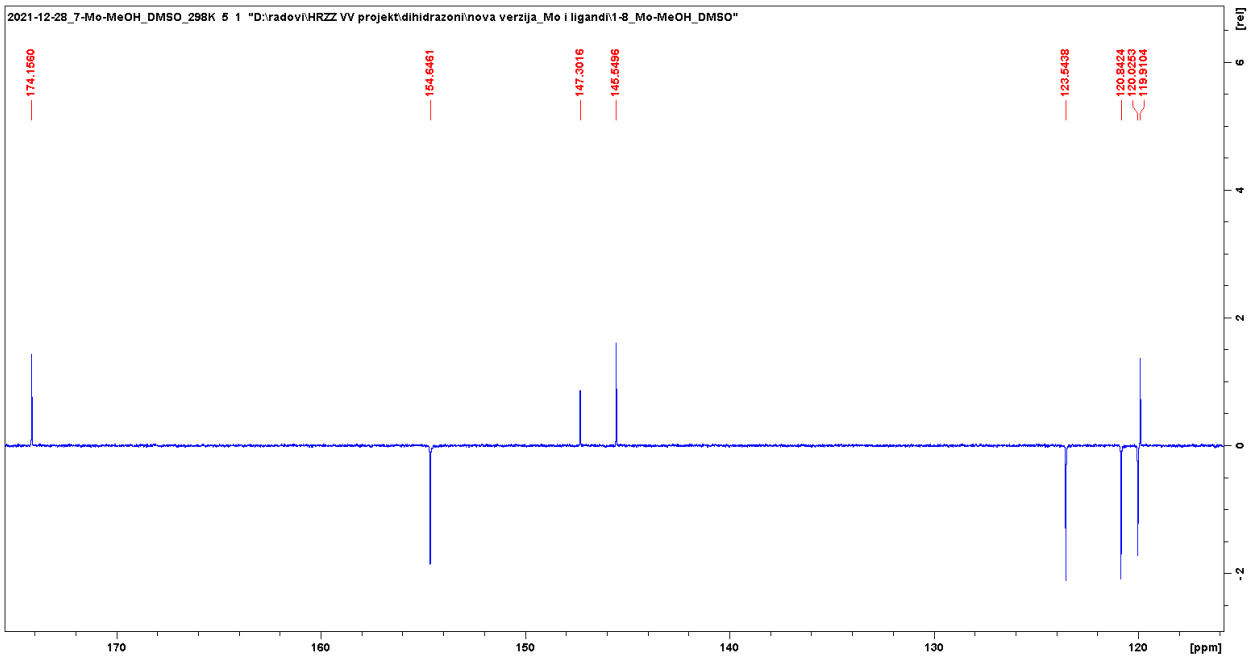

(c)

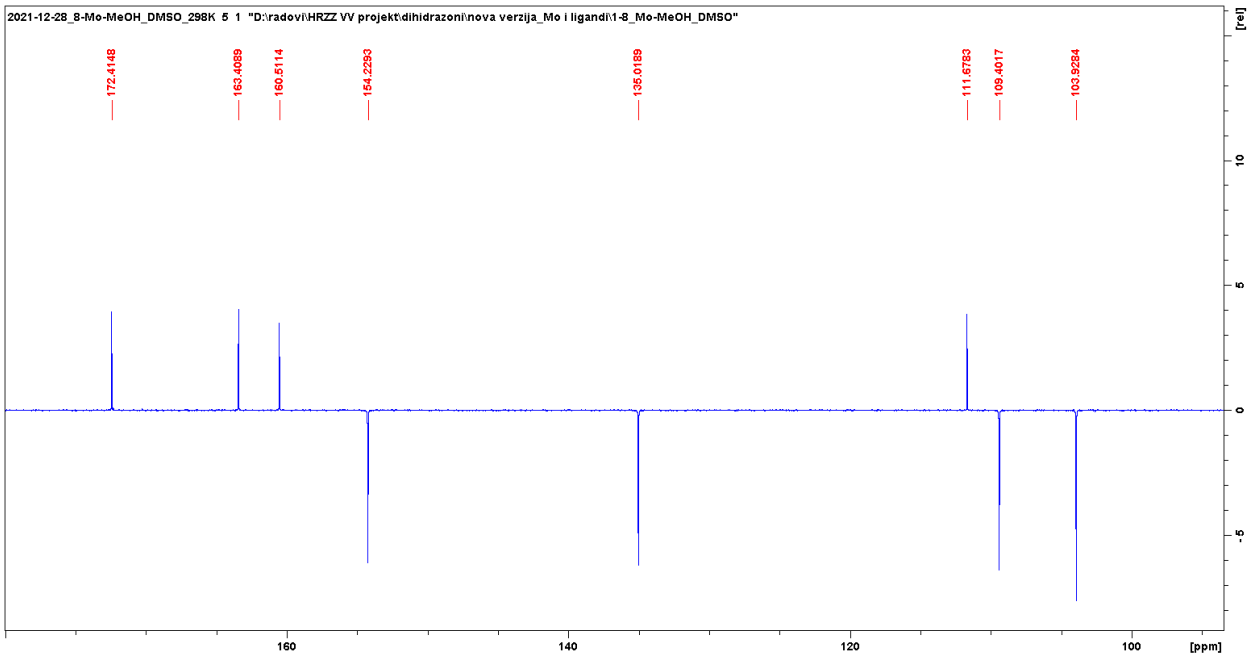

(d)

Figure S31. ^{13}C NMR spectra in selected region for adipoyl-type of complexes: (a) **[$Mo_2O_4(MeOH)_2(L^5)$];** **(b) [$Mo_2O_4(MeOH)_2(L^6)$]**; (c) **[$Mo_2O_4(MeOH)_2(L^7)$]**; (d) **[$Mo_2O_4(MeOH)_2(L^8)$]** in DMSO–d_6 at 298 K.

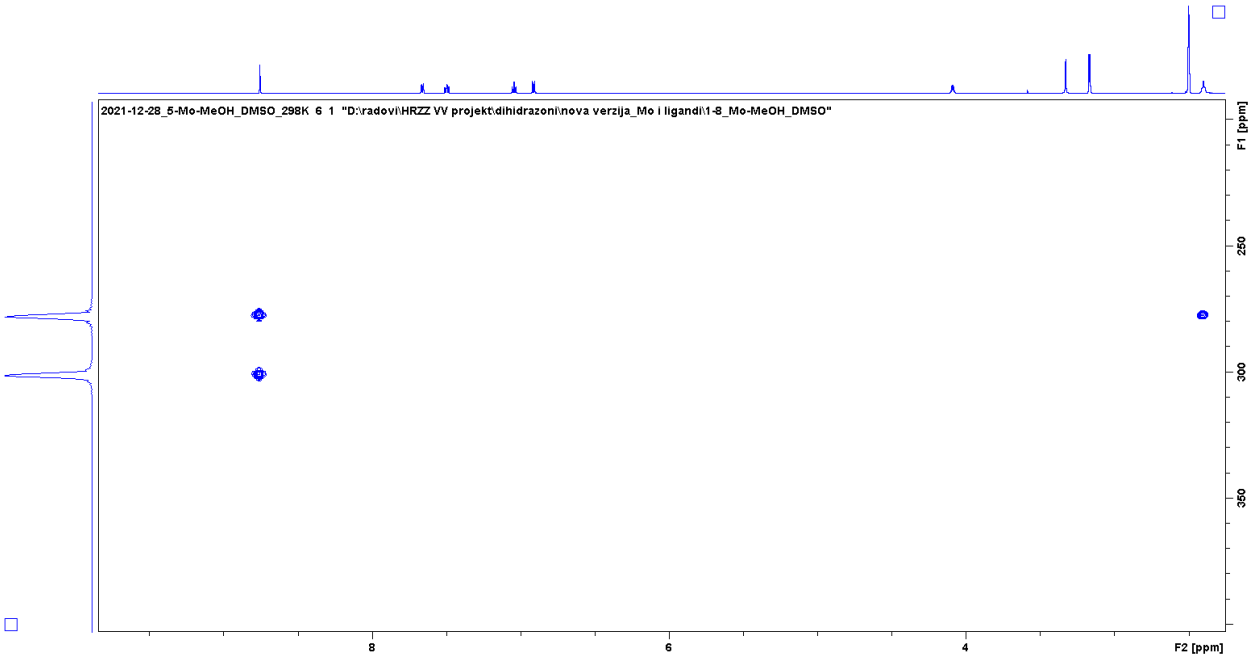
2021-12-28_5-Mo-MeOH_DMSO_298K 6 1 "D:\radovi\HRZZ VV projekt\dihidrazoni\nova verzija_Mo i ligandi\1-8_Mo-MeOH_DMSO"
F1 [ppm]
250
300
350
8
6
4
F2 [ppm]

(a)

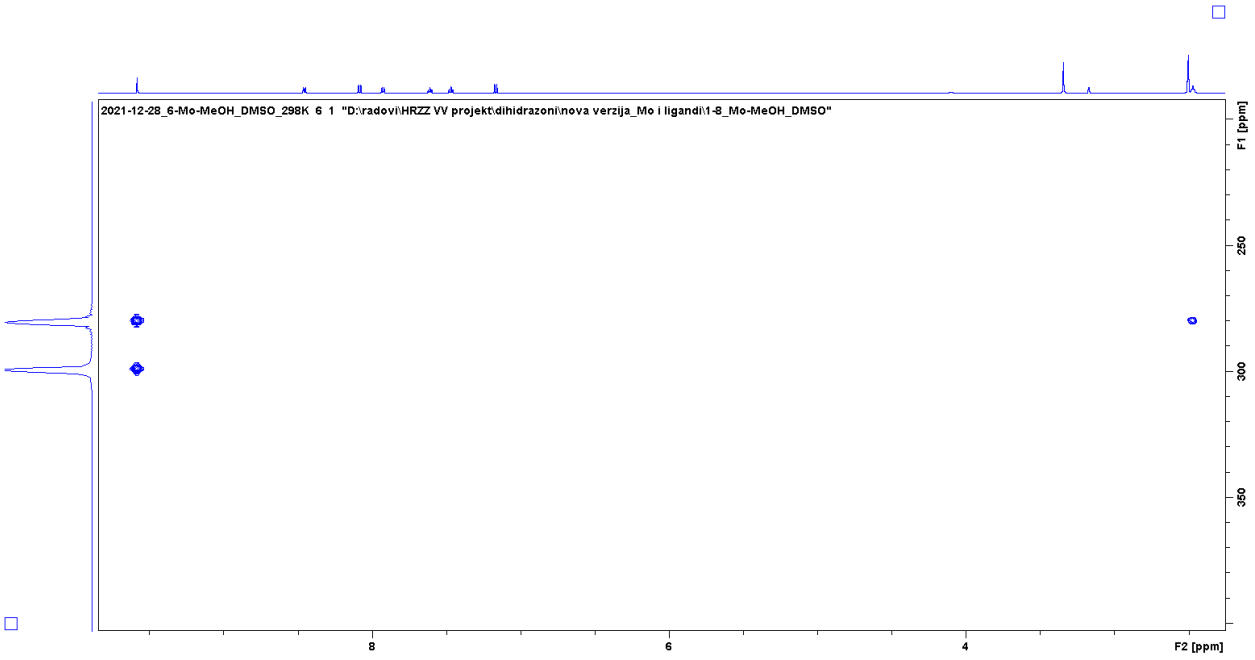
2021-12-28_6-Mo-MeOH_DMSO_298K 6 1 "D:\radovi\HRZZ VV projekt\dihidrazoni\nova verzija_Mo i ligandi\1-8_Mo-MeOH_DMSO"
F1 [ppm]
250
300
350
8
6
4
F2 [ppm]

(b)

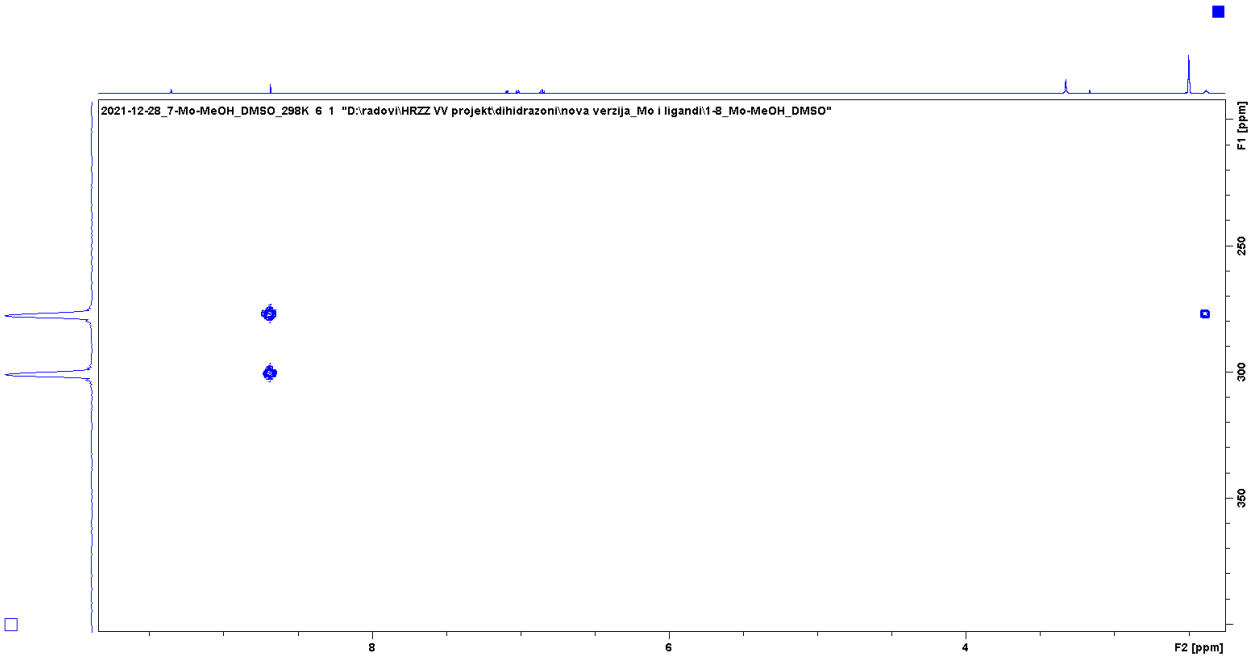

(c)

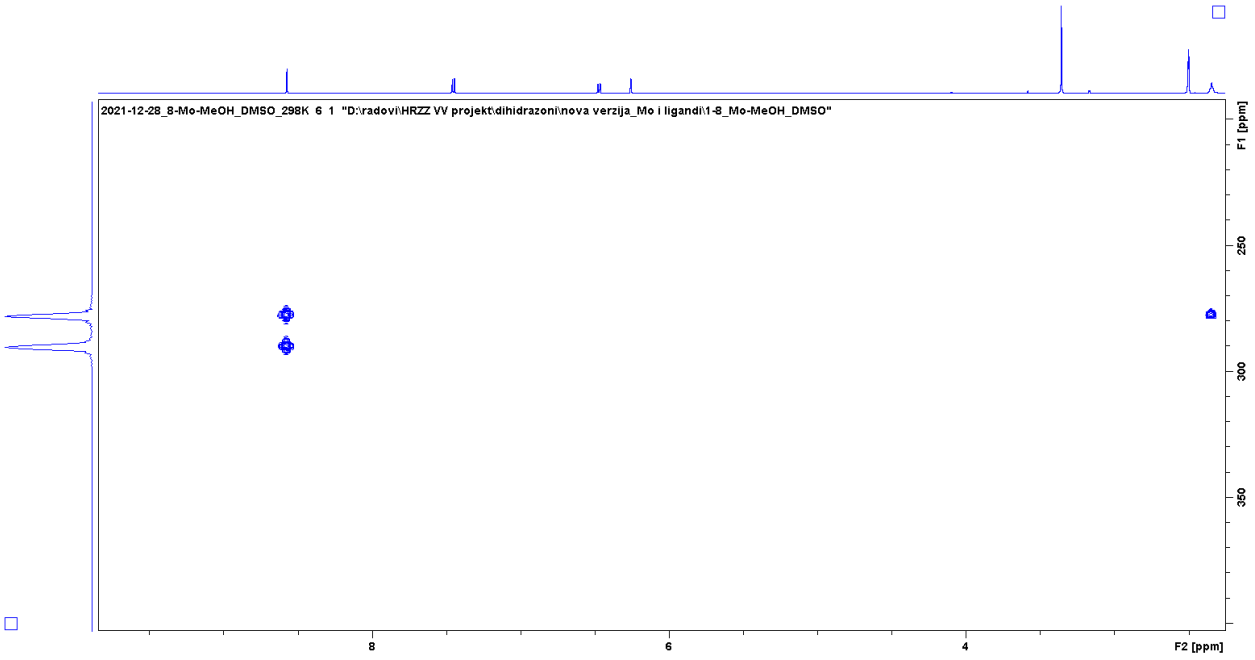

(d)

Figure S32. ^{1}H-^{15}N HMBC NMR spectra in selected region for adipoyl -type of complexes: (a) **[$Mo_2O_4(MeOH)_2(L^5)$]; (b) [$Mo_2O_4(MeOH)_2(L^6)$]**; (c) **[$Mo_2O_4(MeOH)_2(L^7)$]**; (d) **[$Mo_2O_4(MeOH)_2(L^8)$]** in DMSO–d_6 at 298 K.

Table S9. ^{1}H, ^{13}C and ^{15}N chemical shifts for adipoyl-type of complexes (**[Mo$_2$O$_4$(MeOH)$_2$(L^5-L^8)]**) in DMSO–d_6 at 298 K, with the atom numbering scheme

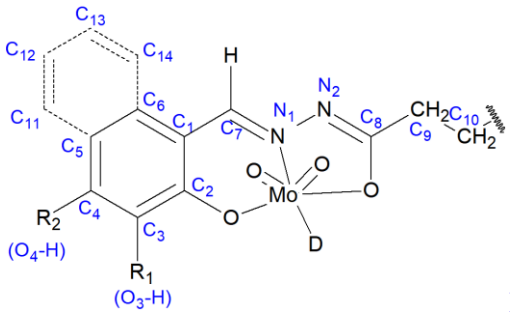

D = MeOH/DMSO

	[Mo$_2$O$_4$(MeOH)$_2$(L^5)]			**[Mo$_2$O$_4$(MeOH)$_2$(L^6)]**			**[Mo$_2$O$_4$(MeOH)$_2$(L^7)]**			**[Mo$_2$O$_4$(MeOH)$_2$(L^8)]**		
atom(s)	δ(^{1}H)	δ(^{13}C)	δ(^{15}N)	δ(^{1}H)	δ(^{13}C)	δ(^{15}N)	δ(^{1}H)	δ(^{13}C)	δ(^{15}N)	δ(^{1}H)	δ(^{13}C)	δ(^{15}N)
1		120.6			129.2			119.9			111.7	
2		159.7			160.7			147.3			160.5	
3	6.91	119.0		7.17	120.8			145.5		6.26	103.9	
4	7.50	135.2		8.09	136.1		7.02	120.0			163.4	
5	7.05	121.9			111.8		6.86	120.8		6.48	109.4	
6	7.66	134.6			132.9		7.09	123.5		7.46	135.0	
7	8.76	155.6		9.58	151.9		8.68	154.6		8.58	154.2	
8		175.4			174.7			174.2			172.4	
9	2.40	31.1			31.1		2.39	30.1		2.35	29.9	
10	1.66	25.8			25.9		1.65	24.7		1.63	24.8	
11				7.93	129.4							
12				7.47	125.1							
13				7.61	128.9							
14				8.46	122.0							
N1			301.0			299.1			300.1			289.1
N2			277.3			280.1			276.3			277.3
O3–H							9.36					
O4–H											10.50	

ATR FT-IR spectroscopy

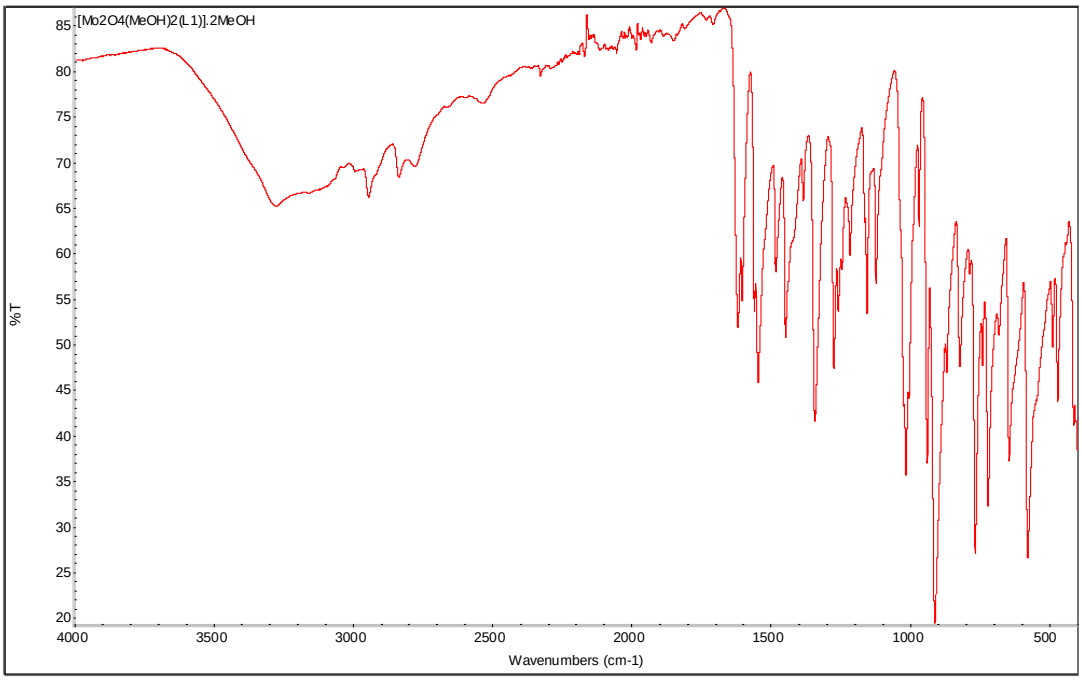

Figure S33. ATR FT-IR spectra of **$[Mo_2O_4(MeOH)_2(L^1)]\cdot 2MeOH$.**

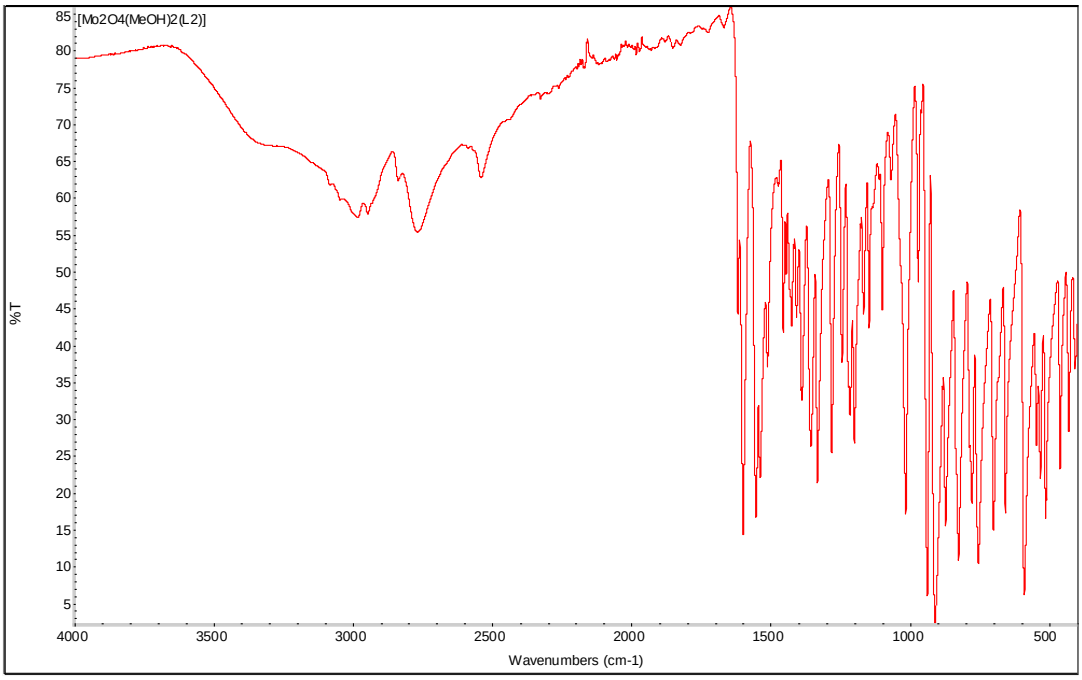

Figure S34. ATR FT-IR spectra of **$[Mo_2O_4(MeOH)_2(L^2)]$.**

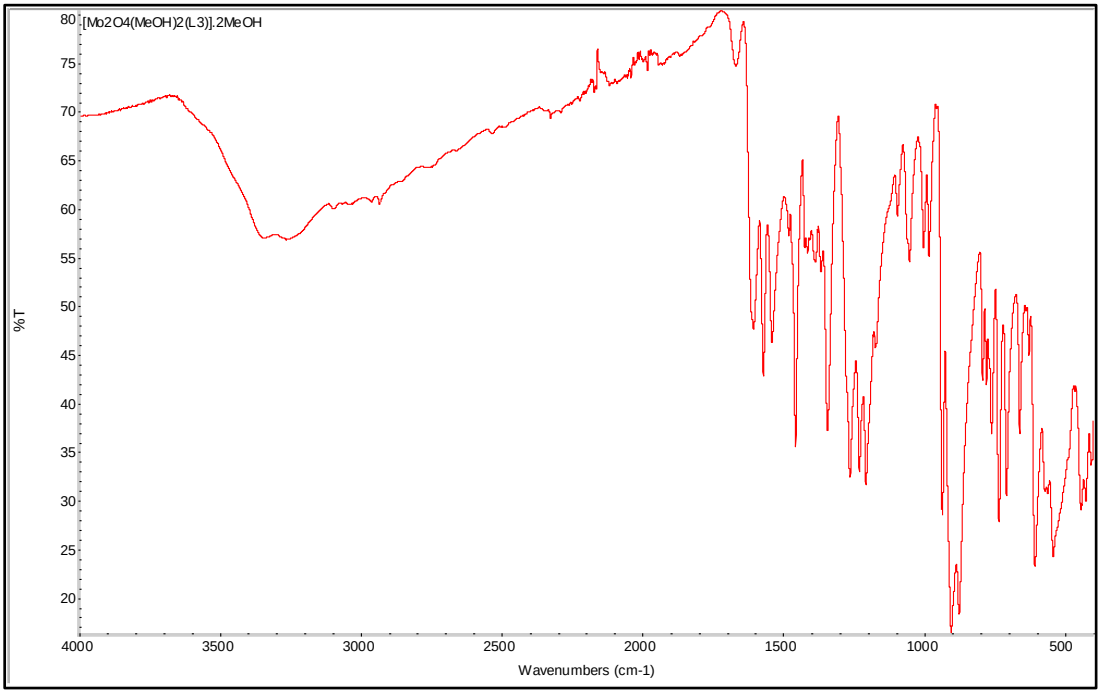

Figure S35. ATR FT-IR spectra of **$[Mo_2O_4(MeOH)_2(L^3)]\cdot 2MeOH$.**

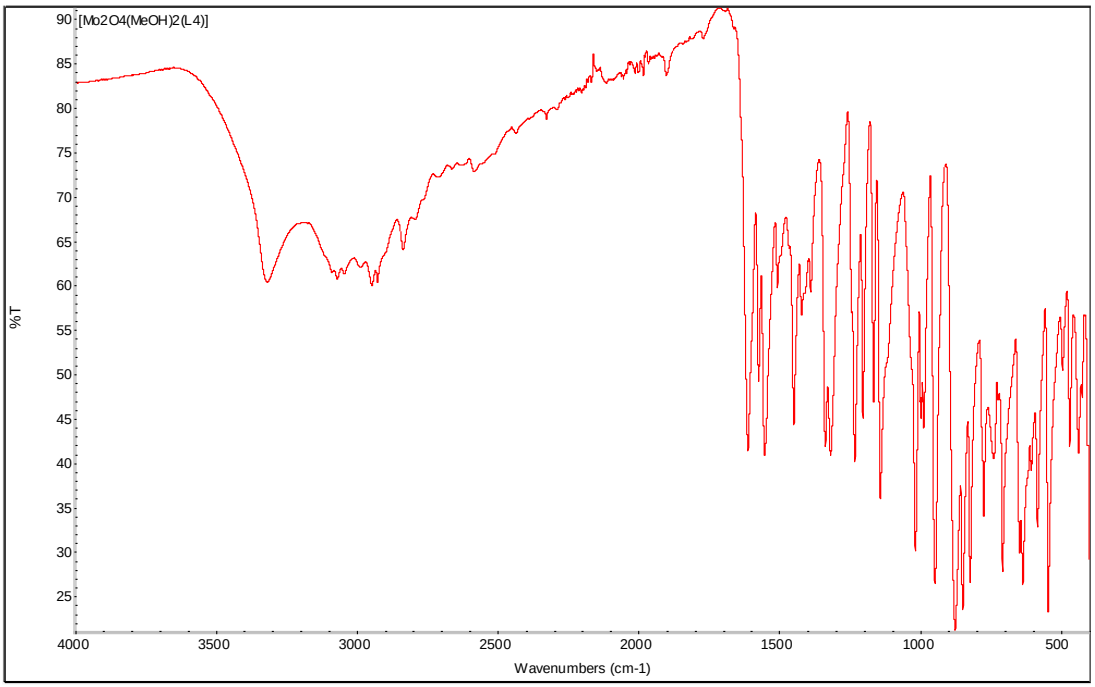

Figure S36. ATR FT-IR spectra of **$[Mo_2O_4(MeOH)_2(L^4)]$.**

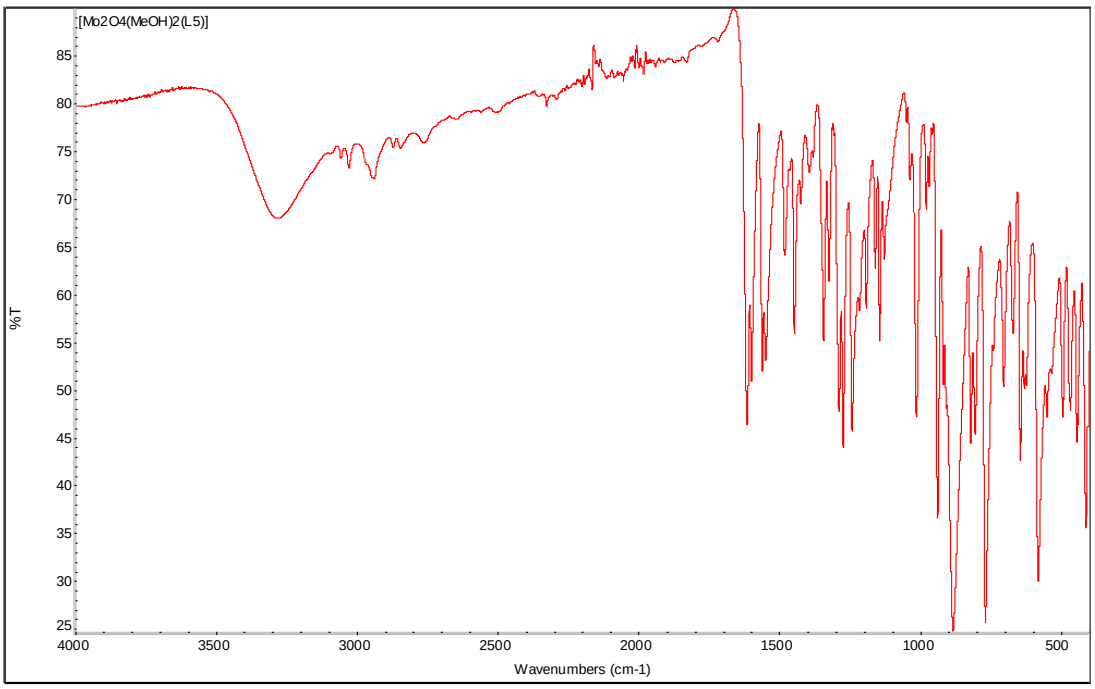

Figure S37. ATR FT-IR spectra of **[$Mo_2O_4(MeOH)_2(L^5)$]**.

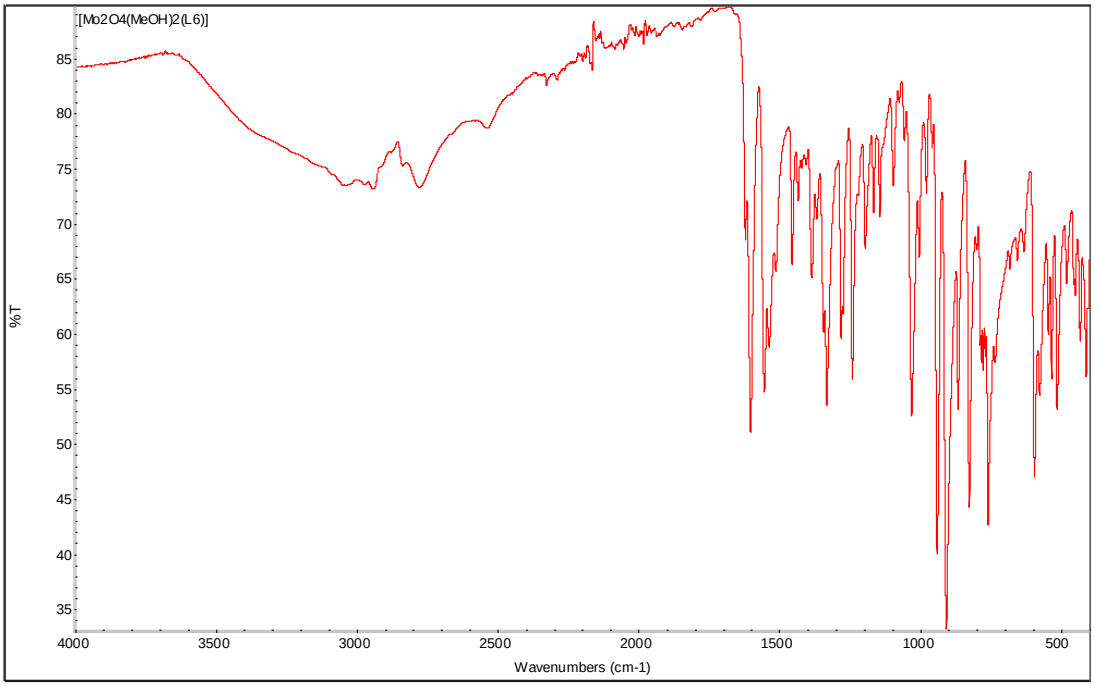

Figure S38. ATR FT-IR spectra of **[$Mo_2O_4(MeOH)_2(L^6)$]**.

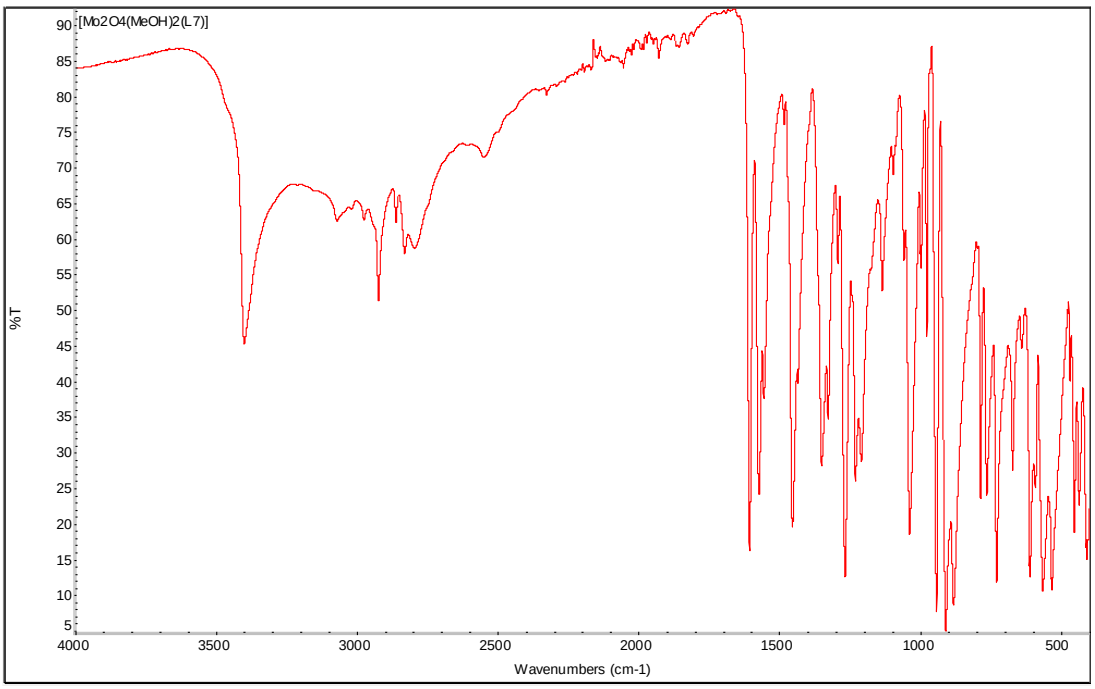

Figure S39. ATR FT-IR spectra of **$[Mo_2O_4(MeOH)_2(L^7)]$.**

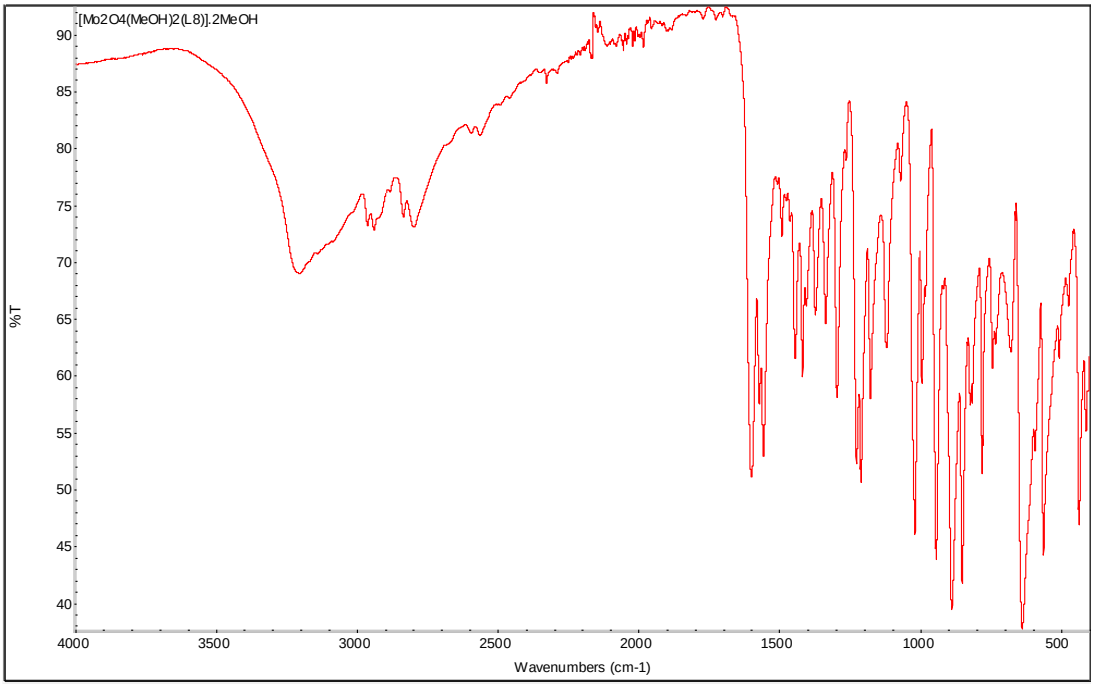

Figure S40. ATR FT-IR spectra of **$[Mo_2O_4(MeOH)_2(L^8)]\cdot 2MeOH$.**